Pathway Specificity of Behavioral Timescale Synaptic Plasticity (BTSP) in The Prefrontal Cortex (PFC)

Somayah Alsayadi

Thesis submitted to the
University of Ottawa
in partial fulfillment of the requirements
for the Master's degree in Neuroscience

Department of Cellular & Molecular Medicine
Faculty of Medicine
University of Ottawa

Table of Contents

List of figures

ABSTRACT

Modern theories of synaptic plasticity, central to understanding learning and memory, suggest that synapses undergo activity-dependent changes in strength. However, traditional models like spike-timing-dependent plasticity (STDP), with their reliance on nearly coincident and repetitive neural activity, fall short of capturing the extended temporal dynamics integral to behavioral learning. This discrepancy presents a notable challenge in synaptic plasticity research, often referred to as the "temporal credit assignment problem," which requires linking actions to outcomes that are temporally separated. Behavioral timescale synaptic plasticity (BTSP) was first discovered in the hippocampus and more recently in the prefrontal cortex of mice. Utilizing a combination of optogenetics and whole-cell electrophysiology experiments we sought to determine BTSP across pathway-specific inputs to layer 5 pyramidal neurons from key brain regions including the ventral hippocampus, basolateral amygdala, mediodorsal thalamus, and contralateral PFC. Our results reveal that BTSP can be selectively induced in the ventral hippocampus-PFC and mediodorsal thalamus-PFC pathways. Additionally, adjustments to *ex vivo* experimental conditions to mirror physiological calcium levels reveal the need for a *Hebbian eligibility trace* in order to induce plasticity. These findings pave the way for future research that bridges cellular mechanisms with behavioral outcomes, offering potential pathways for therapeutic interventions in conditions like Alzheimer's disease, where such synaptic mechanisms are disrupted.

ACKNOWLEDGMENTS

I would like to first extend my profound gratitude to my supervisor, Dr. Jean-Claude Béïque, for his invaluable mentorship, guidance, and unwavering support throughout my research journey. His insights and encouragement have been instrumental in shaping my academic and professional growth. My sincere thanks also go to my advisory committee members, Dr. Katalin Toth and Dr. Richard Naud, for their expert advice and constructive feedback, which significantly enriched my research experience.

Additionally, I am grateful to Dr. Kirk Mulatz and Dr. Érik Harvey-Girard for their technical assistance and input on the project. I would also like to thank all my colleagues and friends in the lab, particularly Dr. Léa Caya-Bissonnette for her incredible guidance throughout this project. Her mentorship has not only equipped me with essential skills and a robust work ethic but has also set a standard of integrity and dedication that continuously drives my pursuit of excellence. The camaraderie and intellectual exchanges within our lab made my research journey highly productive and immensely enjoyable. To my family, whose unwavering support and love have been my cornerstone, I am eternally grateful. Their belief in my abilities and their sacrifices have not gone unnoticed, and I owe much of my success to their unwavering support.

Lastly, I acknowledge the financial support provided by the University of Ottawa, the Province of Ontario, and the government of Canada (National Sciences and Engineering Research Council), which were crucial in facilitating my research and academic endeavors

GENERAL INTRODUCTION

Learning, a cornerstone of adaptive behavior, is not solely a human trait but a fundamental biological process that has evolved across species to enhance survival, growth, and environmental adaptation. At the core of this transformative process lies synaptic plasticity, a dynamic and intricate mechanism within the neural architecture that underpins our ability to learn and remember. Despite the paramount significance of learning for survival and everyday functioning, the nature of synaptic plasticity— the very engine driving our capacity to learn— remains elusive.

The notion that neural connections are subject to modification in response to behavioral experiences traces its roots back to the late 19th century. In 1872, Alexander Bain proposed the coordination of sensations and movements through specific growths in cell junctions (Bain, 1872). This idea gained further traction when American psychologist William James introduced a learning rule akin to Donald Hebb's later hypothesis, emphasizing the propagation of excitement between “active brain processes”(James, 1890). Towards the end of the 19th century, Santiago Ramón y Cajal suggested that memory might be stored through strengthened connections between neurons, a concept later termed synapses by Charles Scott Sherrington in 1897 (Bliss et al., 2018; Ramon Cajal, 1894; Sherrington, 1906).

Alexander Bain proposed that concurrent actions or sensations tend to cohere, facilitating their recall when one is later presented to the mind (Bain, 1855). This early insight laid the foundation for the speculation by future neuroscientists that brain function is governed by associating information(Markram et al., 2011), contributing to our understanding of synaptic plasticity and its role in associative learning.

Synaptic plasticity, the activity-dependent modification of neuronal connections or synapses (Hebb, 1949), forms the basis for learning and memory. According to Hebb’s postulate, when axon A is consistently responsible for postsynaptic firing of cell B, the synaptic strength of this connection is increased (Hebb, 1949). Experimental confirmation came in 1973 through Bliss and Lomo's work on the rabbit hippocampus, introducing the concept of long-term potentiation (LTP) (Bliss & Lømo, 1973a). LTP increases synaptic strength and serves as a potential mechanism

for learning and memory storage. The bidirectional modulation of synaptic strength includes long-term depression (LTD), induced by low-frequency stimulation (Dudek & Bear, 1992). LTD occurs when presynaptic neurotransmitter release doesn't lead to postsynaptic firing, allowing reversibility and preserving information storage capacity (Kennedy, 2016).

Experimental induction of LTP or LTD often involves spike-timing dependent plasticity (STDP) protocols (Markram, Lubke, et al., 1997). However, STDP's temporal requirements (on the order of milliseconds) and repetition rates (50-100) deviate from behavioral associative learning, highlighting a gap between experimental models and real-world scenarios. The concept of an eligibility trace was proposed to address this issue. The eligibility trace is elicited by presynaptic activation and is transformed into LTP by postsynaptic firing, allowing synapses to remain eligible for potentiation over a longer period of time (~1-2 seconds) (Klopf, 1972).

Recent studies by Bittner *et al.*(Bittner et al., 2017) introduce Behavioral Timescale Synaptic plasticity (BTSP) with temporal delays resembling associative learning at longer timescales (1-2 seconds). Their non-Hebbian model, closer to real-world associative learning, suggests that even without postsynaptic spiking, presynaptic inputs create an eligibility trace that, upon postsynaptic firing within a 2-second time window, transforms into LTP. This physiological mechanism aligns with behaviorally relevant contexts, providing insights into synaptic plasticity within a timeframe consistent with associative learning.

Novel findings by Caya-Bissonnette *et al.* (Caya-Bissonnette et al., 2023) reveal BTSP in layer 5 pyramidal neurons of the mouse prefrontal cortex, showcasing synaptic potentiation with behaviorally relevant temporal separations (0.5 s - 1 s). This ground-breaking discovery challenges conventional synaptic plasticity models, adapting to behavioral timescales and introducing a novel mechanism for associative learning, achievable even with a single pairing, resembling one-shot learning. Furthermore, the identification of a distinctive form of short-term and associative plasticity of calcium dynamics (STAPCD) in apical oblique dendrites enhances our understanding of the rules governing BTSP induction.

In this thesis, I extend the groundwork discussed above by delving into the synapse specificity of BTSP within the mouse prefrontal cortex.

1 SYNAPTIC PLASTICITY

In unraveling the complexities of synaptic plasticity, it is paramount to recognize that the brain's function is intricately determined by the connectivity and adaptability of its underlying neurons (Bassi et al., 2019; Kauer & Malenka, 2007). These neural connections possess the remarkable ability to undergo changes and strengthen in response to various experiences, consequently shaping subsequent thoughts and behaviors (Turrigiano & Nelson, 2004). Disruptions in such plasticity have been implicated in the pathogenesis of neuropsychiatric disorders (Kauer & Malenka, 2007).

1.1 SHORT TERM SYNAPTIC PLASTICITY

Short term forms of synaptic plasticity manifest on the order of milliseconds to minutes, reflecting transient alterations in behavioral experiences (Zucker & Regehr, 2002). There are two fundamental facets of short-term plasticity (STP): paired-pulse facilitation (PPF) and paired-pulse depression (PPD) (Katz & Miledi, 1968; Zucker & Regehr, 2002). PPD, often occurring at short interstimulus intervals (ISI <20 ms), is attributed to the transient depletion of the readily releasable pool of vesicles at the presynaptic terminal (Dobrunz & Stevens, 1997). Changes in neurotransmitter release probability or receptor desensitization can also contribute to PPD at longer intervals (~100 ms). On the other hand, PPF, observed at longer ISI's (20 ms-500 ms), is a consequence of residual calcium contributing to additional release upon the second pulse (Dobrunz & Stevens, 1997; Kauer & Malenka, 2007). The occurrence of PPF or PPD is contingent upon the recent synaptic history, driven by changes in release probability (P). Notably, high initial release probability results in PPD, while low probability leads to PPF.

1.2 LONG TERM SYNAPTIC PLASTICITY

Long-term plasticity (LTP) represents a pivotal mechanism in understanding how synaptic strength alterations contribute to behavioral modifications, particularly in learning and memory

formation(Kauer & Malenka, 2007). This phenomenon involves the enduring modification of synaptic weights within a neural circuit, facilitating the storage of information over extended periods. Santiago Ramon y Cajal laid the groundwork for this concept, which was later formalized by Canadian neuroscientist Donald Hebb in 1949 (Hebb, 1949). LTP is characterized by sustained enhancement in synaptic efficacy following high-frequency or repeated stimulation (Bliss & Lømo, 1973a; Martin et al., 2000).

1.2.1 HEBBIAN PLASTICITY

At the core of synaptic plasticity lies the widely acknowledged Hebbian framework, notably illustrated by LTP (Andersen et al., 2017). According to Donald Hebb's postulate, persistent activation of axon A leading to the firing of cell B enhances the synaptic efficacy between the two cells (Hebb, 1949; Figure 1). This implies that presynaptic firing consistently contributing to postsynaptic neuron activation strengthens the synaptic connection over an extended duration. Hebbian LTP and LTD manifest within seconds to minutes, responding to brief episodes of synaptic stimulation, and their effects can endure for hours to days (Abraham & Williams, 2003).

Hebb's postulate was demonstrated experimentally for the first time by Bliss and Lomo's studies on the rabbit hippocampus in 1973 (Bliss & Lømo, 1973b). They induced high frequency (tetanic) stimulations of the perforant path in the dentate area of the hippocampus of anesthetized rabbits. They used recordings of field potentials to measure synaptic responses. This approach allowed them to observe a long-lasting enhancement in the strength of synaptic transmission and larger population spike amplitudes. The phenomena they discovered, termed long-term potentiation (LTP), demonstrated a significant increase in field potential amplitude, which persisted for hours and even weeks, suggesting its potential role in learning and memory processes.

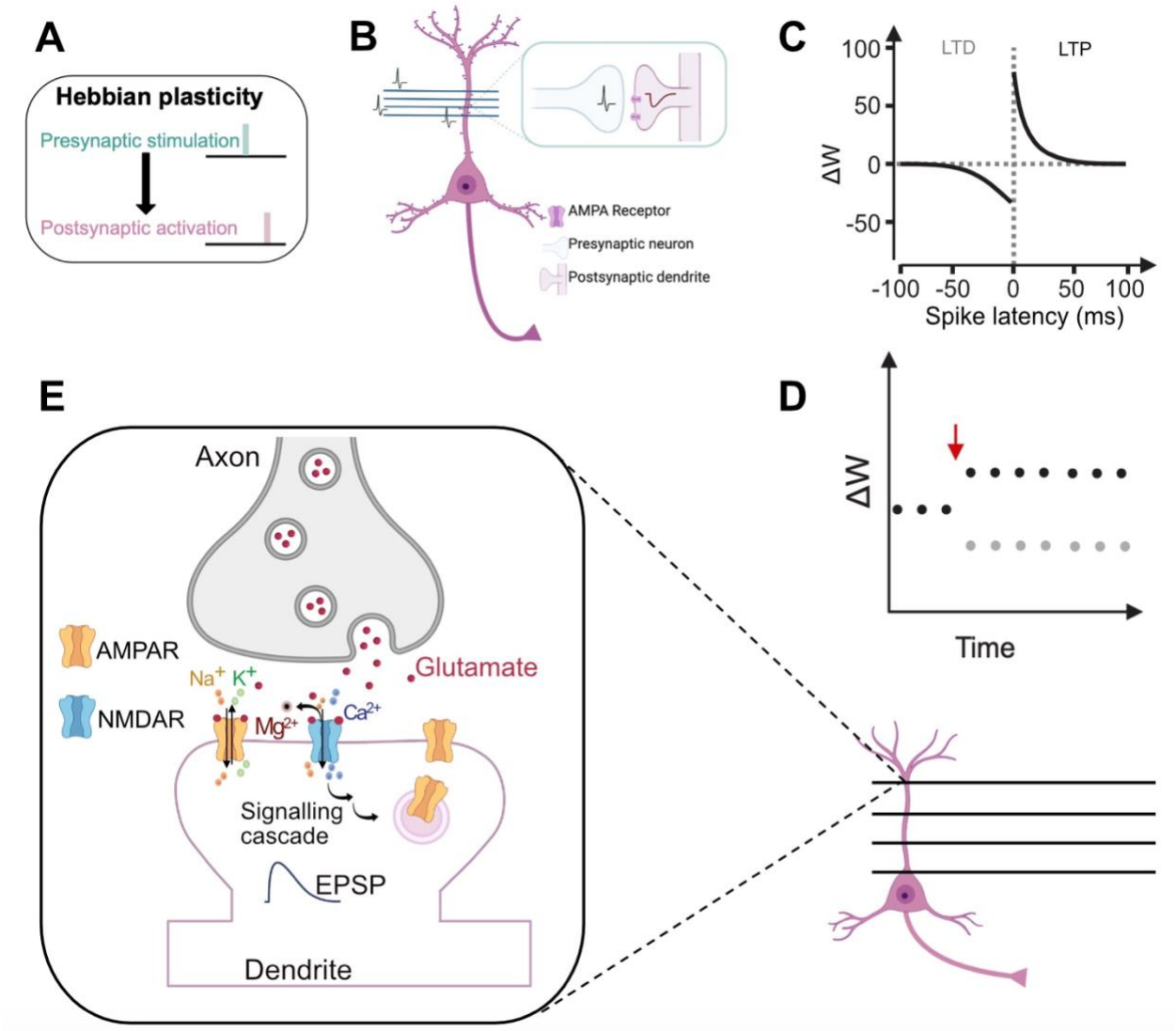

Figure 1. Hebbian plasticity. A) Hebb's postulate: Presynaptic cell A taking part in firing postsynaptic cell B results in strengthening the connection between them. **B)** Schematic of synaptic connection between two neurons. **C)** Schematic representation of Spike-Timing-Dependent-Plasticity (STDP) highlighting 1. The short temporal separation between pre and postsynaptic firing, and 2. The order of activation: if presynaptic cell fires before the postsynaptic cell, long-term potentiation (LTP) occurs, and reversing the order results in depression (LTD). **D)** Synaptic weight is increased during LTP (black) and decreased during LTD (grey). **E)** Close-up illustration of a synapse showing glutamate release and binding to AMPAR and NMDAR postsynaptically. The coincidence of glutamate binding with postsynaptic depolarization (bAPs) relieves the Mg^{2+} block and allows Ca^{2+} entry into the postsynaptic neuron, activating a signaling cascade that results in AMPAR insertion at the synapse, allowing for enhanced synaptic response upon subsequent activity.

1.2.2 NMDAR-DEPENDENT LTP

LTP induction is dependent on N-methyl-D-aspartate receptors (NMDARs), which detect the coincidence of pre- and postsynaptic spiking (Abraham & Williams, 2003; Bock & Stuart, 2016). NMDARs typically consist of two GluN1 and two GluN2 subunits, though this composition can vary as they sometimes also contain GluN3 (Bock & Stuart, 2016). At resting membrane potentials, NMDARs are blocked by a Mg^{2+} ion, preventing the passage of any other ions (Lü Scher et al., 2012). The specific composition of NMDARs determines their biophysical features. For instance, GluN2A- and GluN2B-containing receptors are blocked by Mg^{2+} more strongly than other subunits (Retchless et al., 2012). NMDARs usually have slower kinetics ranging from 40 ms (GluN1/GluN2A) to 2 s (GluN1/GluN2D) (Vicini et al., 1998). NMDAR are activated upon the coincidence of presynaptic inputs (glutamate release) with postsynaptic depolarization. Despite the fact that EPSPs can induce robust postsynaptic depolarization, it is not sufficient for LTP induction (Caya-Bissonnette et al., 2023). Backpropagating action potentials (bAPs) or dendritic spikes are often required to relieve the Mg^{2+} from the NMDAR ion pore (Lisman & Spruston, 2005, 2010; Markram, Lubke, et al., 1997).

The coincidence of glutamate binding to NMDAR with the removal of the Mg^{2+} allows Ca^{2+} ions flow into the postsynaptic cell (Abraham & Williams, 2003). Ca^{2+} influx activates Ca^{2+}-calmodulin-dependent kinase II (CaMKII), resulting in the insertion of more α-amino-3-hydroxy-5-methyl-4-isoxazole propionate receptors (AMPARs) at the postsynaptic dendritic spines (Herring & Nicoll, 2016; Lisman et al., 2002, 2012; Malinow & Malenka, 2003). This increase in AMPAR allows the postsynaptic neuron to be more responsive to subsequent glutamate release, producing a larger postsynaptic response relative to that prior to AMPAR insertion.

AMPARs are tetrameric structures made of combinations of 4 different subunits (GluA1-GluA4) (Castellani et al., 2001; Collingridge et al., 2009). These types of receptors are responsible for the fast synaptic signaling in response to glutamate binding (Dingledine et al., 1999; Llinás et al., 1992; Traynelis et al., 2010). AMPARs mainly conduct sodium (Na^{+}) and potassium (K^{+}) ions and are usually impermeable to Calcium (Ca^{2+}) ions-the GluA2 composition governs their Ca^{2+} permeability (Seeburg & Hartner, 2003). The number/composition of AMPAR on the postsynaptic

membrane is often used to assess modifications in synaptic plasticity (LTP/LTD) (Castellani et al., 2001).

LTP demonstrates four compelling properties that make it an appealing mechanism for learning and memory: persistence, cooperativity, associativity, and input specificity (Nicoll et al., 1988). Synaptic connections exhibiting long-lasting modifications are particularly important for a cellular model of learning and memory storage. Additionally, cooperative interactions between synapses are imperative, necessitating the simultaneous activation of a specific number of presynaptic inputs. Notably, LTP enables the potentiation of weak inputs when paired with strong inputs, emphasizing its role in associativity. Moreover, LTP only occurs in response to the tetanized input and is not found at untetanized inputs to the same cell, which is an optimal feature for information storage (Bliss & Lømo, 1973a; Citri & Malenka, 2007). However, it's essential to acknowledge that while LTP facilitates learning processes, it can also lead to excessive excitability. In this regard, LTD acts as a balancing mechanism, stabilizing synaptic weight to mitigate hyperexcitability induced by LTP (Mulkey & Malenka, 1992; Turrigiano & Nelson, 2004). Despite the elusive nature of the exact mechanism underlying LTD induction, one approach involves low-frequency stimulation (LFS) (Dudek & Bear, 1992).

1.3 SPIKE-TIMING DEPENDENT PLASTICITY (STDP)

Spike-timing-dependent plasticity (STDP) is one proposed mechanism as a cellular model for associative learning (Markram, Lübke, et al., 1997). STDP induction protocols typically involve 50-100 near-simultaneous firing of the pre- and postsynaptic neurons (Bi & Poo, 1998; Debanne et al., 1998; Magee & Johnston, 1997; Markram, Lübke, et al., 1997). Markram *et al.* (1997) found that presynaptic or postsynaptic bursts alone were not sufficient to produce measurable changes in EPSP amplitude (Markram, Lübke, et al., 1997). Their results showed that pairing dendritic/ bAPs with excitatory postsynaptic potentials (EPSPs) is essential for inducing persistent changes in EPSP amplitudes. bAPs therefore serve as a feedback signal to the synaptic input region that an AP had just been fired at the output region (axon) (Magee & Johnston, 1997; Markram, Lübke,

et al., 1997). Bi & Poo, (1998) and Debanne et al., (1998) hypothesized that LTP induction is dependent on the coincidence of NMDAR-mediated EPSP and bAP by postsynaptic depolarization, as opposed to simply the temporal coincidence of pre and postsynaptic firing. This involvement of NMDAR likely gates the critical time window of 50 ms between pre- and postsynaptic activation.

1.3.1 FUNDAMENTAL ISSUES WITH STDP AS A MODEL OF ASSOCIATIVE LEARNING

While the STDP mechanism discussed above seems to be a promising candidate for associative learning, it possesses two fundamental disparities compared to learning observed at behavioral levels (Drew & Abbott, 2006; Suvrathan, 2018). STDP induction protocols require 50-100 pairings, but associative learning rarely takes more than a few repetitions pairing an action with a given outcome. Moreover, the required time window between pre- and postsynaptic activation is on the order of milliseconds, whereas learning at behavioral timescales occurs over seconds, and can be extended to minutes or even hours (Friedrich et al., 2011).

1.3.2 THE ELIGIBILITY TRACE AS A POTENTIAL SOLUTION

Inspired by computational work, a theoretical construct known as an *eligibility trace* has been proposed to address this temporal mismatch, although its biological identity still remains to be identified (Gerstner et al., 2018). This trace is elicited by presynaptic inputs and is transformed into LTP by postsynaptic firing, allowing synapses to remain eligible for potentiation over 1–2 seconds, a timescale consistent with action-reward temporal contingencies observed at the behavioral level (He et al., 2015). He *et al.* (2015) hint at the presence of eligibility traces in the cortex. Their results show that classic STDP protocols used to induce LTP can leave an eligibility trace lasting up to 10 seconds by the neuromodulatory action of norepinephrine (NE) (Gerstner et al., 2018; He et al., 2015).

1.4 BEHAVIORAL TIMESCALE PLASTICITY (BTSP) WITHIN THE HIPPOCAMPUS AND CORTEX

Recent experimental studies by Bittner *et al.* (2017) investigating CA3 to CA1 inputs demonstrate LTP induction even with a temporal separation between pre- and postsynaptic activation on the order of seconds (Bittner et al., 2017; Figure 2A). Their experiments showed that pairing 10 subthreshold presynaptic pulses with postsynaptic depolarization (calcium plateau potential) can induce LTP. This phenomenon is thus thought to be non-Hebbian due to the extended temporal window between pre- and postsynaptic activation, and because presynaptic inputs do not *cause* postsynaptic output. Interestingly, their protocol seems to resemble associative learning more closely as LTP was successfully produced after only 5 pairings, as opposed to the 50 – 100 required by traditional STDP protocols. Additionally, this induction protocol produced LTP even when the temporal delay between pre- and postsynaptic inputs was increased to 1 or 2 seconds. This suggests that, even without eliciting postsynaptic spiking, presynaptic inputs produce an eligibility trace that decays over 2 s. If the postsynaptic cell happens to fire within this timeframe, this eligibility trace is transformed into LTP. Therefore, this study provides a physiologically plausible mechanism that addresses associative learning at behaviorally relevant contexts (timescale and pairing repetitions).

Caya-Bissonnette *et al.* (2023; Figure 2B) unveil a variant form of BTSP in layer 5 (L5) pyramidal neurons in the mouse prefrontal cortex (PFC) through methodologies combining whole-cell recordings, calcium imaging, and biophysical modeling (Caya-Bissonnette et al., 2023). Synaptic potentiation was observed with temporally separated pre- and postsynaptic events, irrespective of order. The endoplasmic reticulum (ER) is presented as a key player in the latent *eligibility trace*. This trace retains the memory of the initial stimulation preceding the arrival of the second stimulation by elongating the decay time constant of calcium. These findings elucidate a novel mechanism for synaptic weight updates upon delayed instructive signals, providing a cellular model of reinforced learning.

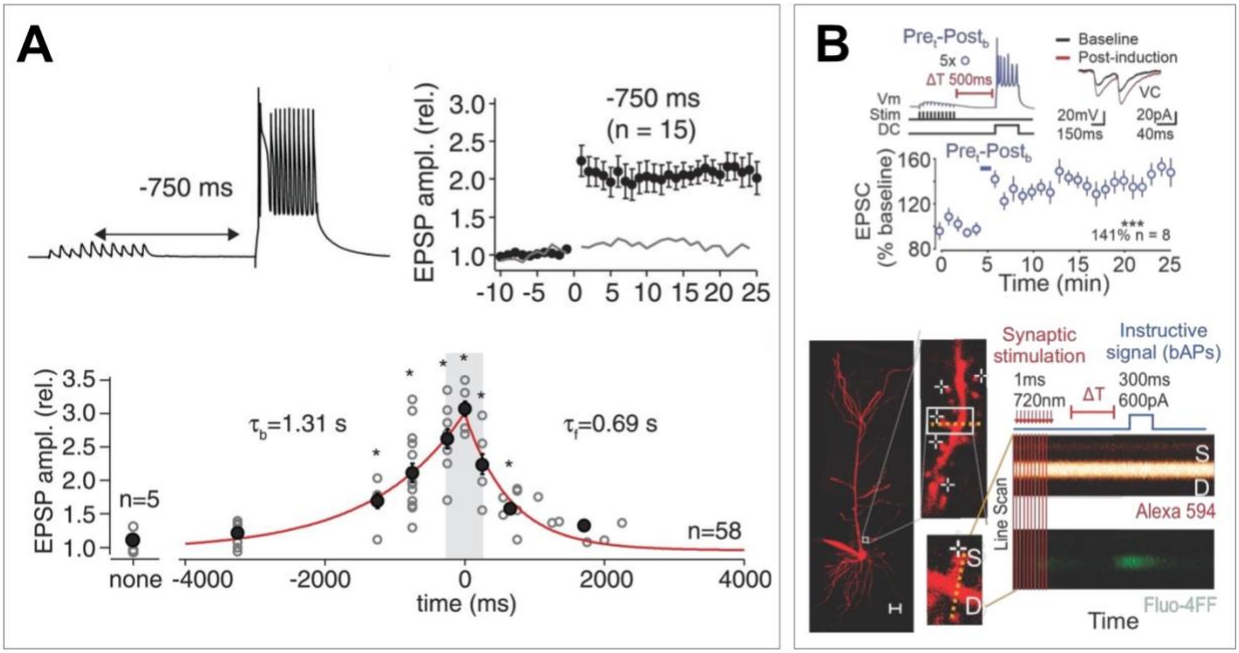

Figure 2. The initial reports of behavioral timescale plasticity (BTSP). A) The first documentation of BTSP in the hippocampus by Bittner *et al.* (2017). Top panel shows the BTSP induction protocol of 10 synaptic stimuli (20 Hz), followed by current injection (300 ms) to mimic plateau potentials. The plot on the right shows average EPSP amplitudes during baseline (first 10 minutes) and following 5 pairings of BTSP induction protocol. Bottom panel shows the bidirectional temporal profile of BTSP. **B)** The first documentation of BTSP in the prefrontal cortex by Caya-Bissonnette *et al.* (2023). Top panel shows a similar BTSP induction protocol (10 synaptic stimuli @ 20 Hz followed by current injection for 300 ms) on Layer 5 pyramidal neurons. This induction protocol results in 41% increase in EPSC amplitude relative to baseline. Bottom panel shows two-photon uncaging experiments paired with calcium imaging. Results reveal a boost of calcium influx when bAPs are preceded by activation of clustered synaptic inputs in a timescale that is consistent with BTSP.

2 THE PREFRONTAL CORTEX AS AN ASSOCIATION CORTEX

The PFC is crucial for orchestrating the top-down control of various cognitive functions to support adaptive behavior (Euston et al., 2012; Twining et al., 2020). It is also a vital hub interconnecting various brain regions, including sensory association cortices, the limbic system, other cortical areas, and the dorsomedial nucleus of the thalamus (Rose & Woolsey, 1949). As a principal integration center, the PFC processes somatosensory inputs from these diverse sources. Structurally, it comprises three main regions: the dorsal, medial, and ventral segments, with the dorsolateral region specializing in higher-order cognitive processing, while the medial and ventral

regions regulate emotions and memory via communication with the limbic system (Anastasiades & Carter, 2021). Within the medial PFC, divisions along the ventral-dorsal axis delineate distinct areas, including the infralimbic (IL), prelimbic (PL), and anterior cingulate cortex (ACC) (Anastasiades & Carter, 2021; Van De Werd et al., 2010). Its distinct architecture is characterized by the absence of a thalamo-receiving layer 4 (L4) and the presence of input-receiving layers L1, L2/3, L5, and L6 (Anastasiades & Carter, 2021). Importantly, the mPFC receives a variety of long-range excitatory inputs from several brain regions and integrates association inputs. "These inputs notably include connections from the ventral hippocampus (vHIP), basolateral amygdala (BLA), and mediodorsal thalamus (mdTh) (Collins et al., 2018; Hoover & Vertes, 2007; Kelly & Martina, 2018; Liu & Carter, 2018a; Manoocheri & Carter, 2022). Understanding how synaptic inputs from diverse afferents are integrated within the mPFC is essential for elucidating the cellular mechanisms that govern its function, especially as a higher-order cognition and association area.

2.1 BLA-mPFC

The basolateral amygdala (BLA) is integral to the limbic system, which regulates emotional processes, including anxiety and fear (Yang & Wang, 2017). The BLA, particularly its subregions, directly projects to the medial prefrontal cortex (mPFC), a critical area for emotional response regulation, decision-making, and cognitive control (Herry et al., 2008; Little & Carter, 2013). Studies have highlighted strong reciprocal connectivity between these regions, with BLA inputs preferentially targeting L5 pyramidal neurons in the mPFC, affecting both the prelimbic (PL) and infralimbic (IL) areas differently (Manoocheri & Carter, 2022).

They found that BLA inputs targeted L5 CA neurons more proximally than CC neurons. Experiments focused on anatomic labeling suggest differential targeting from the BLA to PL or IL regions of the PFC (Kim et al., 2016). Manoocheri *et al.* (2021) further found that the rostral region of the BLA (rBLA) preferentially targets the PL and the caudal BLA (cBLA) projects to the IL. They also utilized *ex vivo* recordings and optogenetics to study this connectivity in more detail. Their results showed that rBLA projects to both L2 and L5 of the PL and cBLA afferents are restricted to IL L5. rBLA inputs target basal dendrites and the cBLA target peri-somatic dendrites of PL L2 and

IL L5 neurons, respectively. There was no rBLA projections to apical or basal dendrites of PL L5 neurons.

The primary function of the amygdala is to process emotional information, especially in the context of fear (Gale et al., 2004). Various behavioral studies revealed the BLA's role in both acquisition and expression of conditioned fear response and associative fear memories (Dilgen et al., 2013; Gale et al., 2004). The BLA-mPFC pathway has been implicated in mediating anxiety, goal-directed social behavior, and the formation of emotional memories (Bechara et al., 1999; Felix-Ortiz et al., 2016; Gale et al., 2004; Ghods-Sharifi et al., 2009). The study by Felix-Ortiz et al. (2016) demonstrates the role of BLA projections to the mPFC in regulating anxiety-like phenotypes as well as social behavior in mice. While activating the BLA-mPFC pathway was found to produce anxiogenic effects and reduce social interaction, photoinhibition of BLA terminals in the mPFC elicited the opposite effects where it reduced anxiety-like behavior and increased social behavior.

In clinical contexts dysfunction of these connections contributes to a number of neuropsychiatric disorders, such as PTSD and depression (Felix-Ortiz et al., 2016; Gilboa et al., 2004; McTeague et al., 2020). Neuroimaging studies in humans further show heightened activity in the BLA in a number of anxiety conditions (Rauch et al., 2003). Zhang *et al.* examined the BLA-PFC functional connectivity in depressed patients and found that the diseased group had a statistically stronger connectivity between the two regions compared to the healthy counterparts (Zhang et al., 2020). This increase was even reduced following 8 weeks of antidepressant treatment. This intricate network between the BLA and mPFC underscores its significance not only in normal cognitive and emotional processing but also in the pathology of mental health disorders, highlighting its potential as a target for therapeutic interventions.

2.2 cPFC-mPFC

Neurons within the prefrontal cortex project contralaterally to the other hemisphere, facilitating interhemispheric communication critical for coordinating complex behaviors (Anastasiades & Carter, 2021). These projections target intratelencephalic-type (IT) cells across all

layers, with a notable bias towards layer 5 pyramidal tract (PT) over layer 5 intratelencephalic (IT) cells, similar to inputs from the amygdala (Lee et al., 2014; Little & Carter, 2013). Despite extensive contact, cPFC axons exhibit no preferential connectivity between callosal-associational (CA) and corticocortical (CC) cells, suggesting a versatile role in integrating and relaying information across the cortex (Anastasiades & Carter, 2021).

Disruptions in these commissural connections have been implicated in various neuropsychiatric disorders. For example, abnormal activity and structural changes in these pathways have been observed in conditions such as schizophrenia and bipolar disorder, where they may contribute to cognitive dysfunctions and altered interhemispheric communication (Parnaudeau et al., 2018). Neuroimaging studies often show altered activation patterns in these regions during tasks that require interhemispheric coordination, underscoring their importance in maintaining cognitive and emotional balance.

Understanding the role of cPFC-mPFC pathways not only illuminates aspects of cognitive processing and behavioral regulation but also highlights potential therapeutic targets for enhancing interhemispheric communication in mental health disorders.

2.3 vHIP-mPFC

The ventral hippocampus (vHIP) provides significant long-range glutamatergic inputs to layer 5 (L5) pyramidal neurons in the medial prefrontal cortex (mPFC), originating primarily from the CA1/subiculum regions (Barbas & Blatt, 1995; Gabbott et al., 2005; Hoover & Vertes, 2007; Liu & Carter, 2018a; Thierry et al., 2000). Those unidirectional connections are crucial for memory formation and storage and are disrupted in neuropsychological disorders such as schizophrenia (Dembrow et al., 2010; Godsil et al., 2013; Siapas et al., 2005; Thierry et al., 2000). Neural synchrony studies between these regions have demonstrated theta rhythm phase locking, highlighting a temporal lag that suggests the directionality of this pathway (Siapas et al., 2005). Intriguingly, most hippocampal inputs to the mPFC originate almost exclusively from its ventral region, targeting both L2/3 and exclusively L5 of the IL and PL regions of the mPFC, respectively (Kelly & Martina, 2018; Liu & Carter, 2018b).

Projections to the IL cortex are thought to be important for the recall of fear memory extinction(Brockway et al., 2023; Marek & Sah, 2018; Milad & Quirk, n.d.; Peters et al., 2010) . Liu & Carter (2018) demonstrate that these inputs undergo facilitation at higher frequencies, indicating enhanced activation within the cortex. It's worth noting that the hippocampus shares with the PL cortex the function of contextual processing and working memory (Twining et al., 2020). As such, it is hypothesized that the prelimbic cortex integrates inputs from the vHIP to regulate the expression of fear memories based on contextual cues (Burgos-Robles et al., 2009; Twining et al., 2020) Twining *et al.* (2020) suggest that the vHIP continuously updates the PL of the animal's state, allowing for aversive memory contextual associations. Tripathi *et al.* (2015) further demonstrate the induction of LTP following high frequency stimulation of this pathway, results that were also found by Laroche *et al.* (1990) in anesthetized and awake rats.

The PFC is often considered responsible for controlling executive functions such as working memory and decision making (Miller & Cohen, 2001). Additionally, it is important for long term memory consolidation and regulation of emotional responses, especially those linked to fear and anxiety (Euston et al., 2012; Heidbreder & Groenewegen b, 2003; Tovote et al., 2015). This allows the animal to not only adaptively anticipate danger but also extinguish the fear response when the threat is gone. The hippocampus is also classically involved in the formation of new memories (Squire, 1992). vHIP projections to the mPFC are implicated in encoding memory and emotional valence (Padilla-Coreano et al., 2016; Spellman et al., 2015). Spatial working memory (SWM) is the ability to store spatial locations in short term memory, which also requires coordination between both the hippocampus and the PFC (Dudchenko, 2004). This was further confirmed by lesion studies that demonstrated hippocampus and PFC interactions during SWM (Yoon et al., 2008).

One human study recorded neural activity from the hippocampus and PFC of a patient during epilepsy surgery. Interestingly, the authors found that hippocampal-prefrontal synchrony was strengthened during a facial working memory task, and it got even stronger as the working memory load was increased by adding the number of items to be remembered (Axmacher et al., 2008). fMRI studies also confirm this finding that working memory tasks are correlated with increased functional connectivity between the two regions (Finn et al., 2010).

In a broader context, this interaction between the hippocampus and the prefrontal cortex has been implicated in a number of psychiatric disorders (Tripathi et al., 2016). Benetti et al. (2009) found that disruptions of this pathway could indicate vulnerability to developing psychosis, hinting that defective connectivity between the hippocampus and the prefrontal cortex might contribute to the cognitive symptoms seen in schizophrenic patients(Benetti et al., 2009). Its role in contextual fear cues also makes it an interesting pathway to study when looking at trauma recovery in post-traumatic stress disorder (PTSD) patients (Yehuda & LeDoux, 2007).

2.4 mdTh-mPFC

The mediodorsal thalamus (mdTh) is a key thalamic nucleus projecting primarily to the prefrontal cortex (PFC), playing a crucial role in cognitive processes beyond traditional sensory relay functions (Parnaudeau et al., 2018; Schmitt et al., 2017; Thierry et al., 2000). The thalamus has classically been viewed as the brain region responsible for relaying sensory information from the periphery to the cortical areas (Guillery & Sherman, 2002). However, it is worth noting that the mdTh has limited connectivity with sensory areas and is rather more heavily connected to the PFC (Parnaudeau et al., 2018). Interestingly, the PFC and the mdTh both play a role in cognitive processing as shown by similar cognitive dysfunctions following lesions of either region (Bradfield et al., 2013; Mitchell & Chakraborty, 2013).

This connectivity has been hypothesized to mediate working memory and behavioral flexibility as seen by a number of lesion studies (Chauveau et al., 2005; Floresco et al., 1982; Hunt & Aggleton, 1991; M'harzi et al., 1991; Parnaudeau et al., 2013; Young et al., 1996). Another function the mdTh-mPFC pathway has been implicated in is behavioral flexibility. This defines an animal's ability to modify their behavior and adjust to constant changes within their environment (Parnaudeau et al., 2018). An example of this function is seen in set-shifting tasks where subjects shift back and forth between a variety of mental tasks (Irwin et al., 2019). Another one is during reversal learning, where reward related contingencies are reversed, requiring individuals to adjust their behavior accordingly (Izquierdo et al., 2017).

Collins *et al.* (2018) studied the long-range connectivity between the mediodorsal and the ventral thalamic nuclei and the PFC. They found that mdTh axons target distinct cell types in superficial and deeper layers in the PFC. It is well known that the mPFC and the mdTh are reciprocally connected. Moreover, the researchers explored whether mdTh inputs also connect with other neuronal populations beyond the corticothalamic (CT) neurons. Another group is the corticocortical (CC) neurons which span multiple layers and project to the contralateral PFC (cPFC). They first confirmed that the CT and CC groups do in fact represent two distinct cell groups by recording from those cells in L5. They performed optogenetic experiments and recorded thalamic inputs in CT and CC neurons and, to their surprise, found stronger inputs at L5 CC neurons. It is also hypothesized that mdTh-CT inputs are likely more distal, as evident by slower EPSC decay kinetics (Marlin & Carter, 2014; Spruston et al., 1994). mdTh inputs preferentially target the soma and proximal dendrites of L5 CC neurons, whereas mdTh-L5 CT projections peak at distal apical dendrites.

Clinically, disruptions in this pathway are implicated in neuropsychiatric disorders like schizophrenia, where deficits in working memory and behavioral flexibility are prominent symptoms (Forbes et al., 2009; Parnaudeau et al., 2013). Human imaging studies demonstrate decreased mdTh activity when performing cognitive tasks (Minzenberg et al., 2009). The extensive reciprocal connections between the PFC and the thalamus render the mdTh an interesting candidate to study cognitive symptoms. The main symptoms seen by disrupting this connection are deficits in working memory and behavioral flexibility (Forbes et al., 2009; Parnaudeau et al., 2018). Thalamocortical functional connectivity is also impaired in major depressive disorder (Brown et al., 2017). As such, enhanced understanding of this pathway can enhance clinical knowledge about certain disorders and cognitive deficits and potentially serve as the starting point for promising therapeutic approaches for patients with mental disorders.

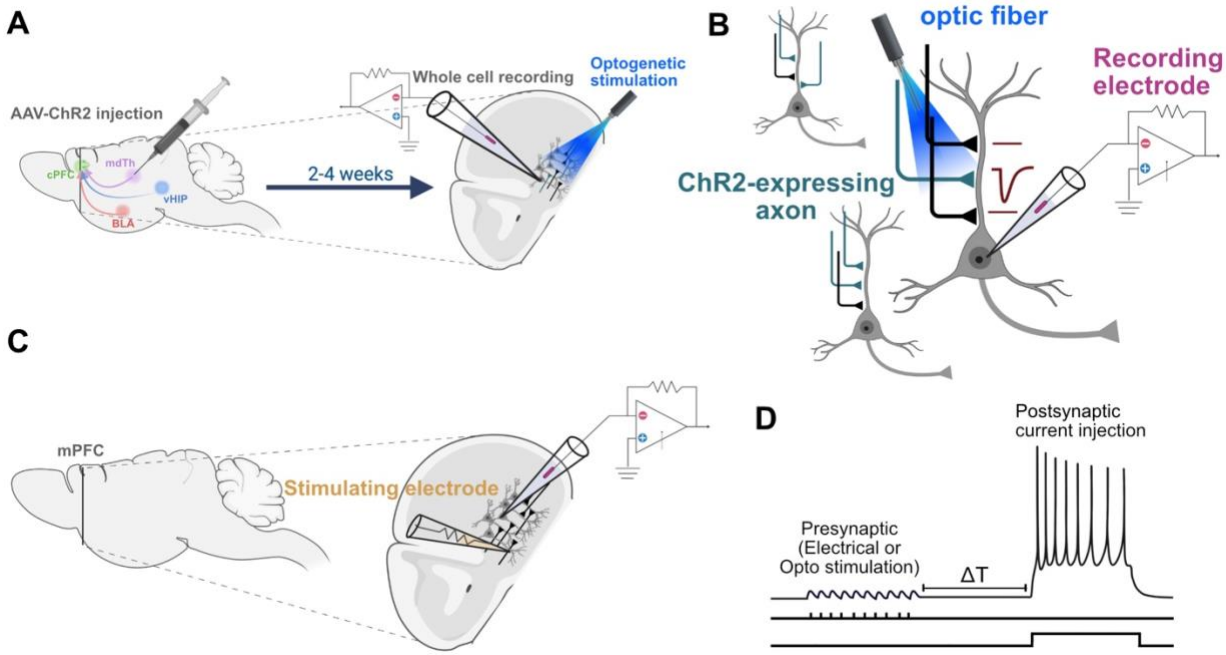

Figure 3. Experimental methods. A) AAV-mediated delivery of ChR2 in the brain region of interest, followed by a waiting period of 2-4 weeks for viral expression. Acute slices were then prepared for whole-cell electrophysiology experiments. **B)** Schematic of the optogenetic stimulation approach and electrophysiological recording setup. ChR2-expressing axons (teal) respond to LED stimulation, eliciting EPSCs. The recording electrode allows for the measurement of neuronal responses to optogenetic stimulation. Non-ChR2 containing axons (black) do not respond to LED stimulation. **C)** Schematic of the electrical stimulation approach where a stimulating electrode is placed proximal to L5 neuron apical dendrites and a whole-cell patch electrode is used to record activity from neurons. **D)** BTSP induction protocol. A train of 10 synaptic inputs (pre; 20 Hz) is delivered prior to bAPs (post) induced via current injection (usually 600 pA for 300 ms). ΔT refers to the temporal window separating pre and post inputs.

2.5 BTSP rules under physiological conditions

Despite robust evidence supporting the role of Long-Term Potentiation (LTP) in learning and memory, many electrophysiology experiments employ conditions that do not mimic the in vivo environment, particularly concerning calcium (Ca^{2+}) levels (Bi & Poo, 1998; Debanne et al., 1998; Markram et al., 2011; Markram, Lübke, et al., 1997; Tse et al., 2007). Typically, artificial cerebrospinal fluid (ACSF) used in *ex vivo* experiments contains abnormally high Ca^{2+} concentrations (2-3 mM), compared to the physiological levels observed *in vivo* (1.2 – 1.8 mM) (Jones & Keep, 1988; Silver et al., 1990). It is important to note that these concentrations do vary

with the sleep-wake cycle and with age. Inglebert et al. (2020) demonstrated that under physiologically relevant Ca^{2+} concentrations, traditional STDP was absent, only to be restored by high-frequency bursting, not by single spike pairings.

Given that long-term potentiation (LTP) induction protocols rely on backpropagating action potentials, calcium plays a pivotal role in these mechanisms (Bi & Poo, 1998; Debanne et al., 1998; Markram, Lübke, et al., 1997). Elevated levels of extracellular calcium are advantageous as they stabilize synaptic recordings and inhibit intrinsic bursting, which could otherwise disrupt spike-timing-dependent plasticity (STDP) induction (Forsberg et al., 2019). However, such experimental enhancements could distort our understanding of synaptic plasticity dynamics as they naturally occur, potentially overestimating the magnitude of plasticity observed during actual learning processes. This discrepancy raises important considerations for interpreting experimental data in the context of natural neural function.

3. Objective

Given the complex architecture and functional diversity of the prefrontal cortex (PFC), it is crucial to investigate how different synaptic inputs, originating from distinct brain regions with varied functions, comply with or diverge from established Behavioral Timescale Synaptic Plasticity (BTSP) rules. Achieving this understanding is essential if we want to elucidate how the brain integrates and processes information at a cortical level. This exploration will allow us to dissect the mechanisms by which the PFC coordinates higher cognitive functions such as decision making, emotional regulation, and problem-solving, revealing how synaptic integration and plasticity within these networks shape behavioral outputs.

4. Results

4.1 Amygdalar inputs onto mPFC L5 neurons do not undergo BTSP

Building on prior research by Caya-Bissonnette et al. (2023), we explored pathway-specific BTSP rules within the mPFC. Acute mPFC brain slices were prepared for whole-cell electrophysiology recordings from L5 pyramidal neurons in both male and female mice. Picrotoxin (PTX) was added to the potassium (K)-Gluconate intracellular solution to isolate excitatory postsynaptic currents (EPSCs) and inhibit GABAA currents.

For targeted study of the BLA-mPFC pathway, AAV-ChR2-mCherry was bilaterally injected into the BLA of SERT-CRE mice. Following a 2-4 week period for viral expression, we performed *ex vivo* slice recordings. Optogenetic stimulation with brief light pulses (1-2 ms) resulted in glutamate-driven EPSCs (**Figure 3**).

To confirm that these connections were monosynaptic, we applied Tetrodotoxin (TTX), which blocked all sodium-dependent action potentials, effectively silencing all synaptic activity. This intervention resulted in the disappearance of these EPSCs, indicating their reliance on action potential propagation. Subsequent application of 4-aminopyridine (4-AP), which blocks potassium channels and enhances depolarization, restored these EPSCs upon light stimulation. The restoration of EPSCs specifically by 4-AP, even in the presence of TTX, confirms that the EPSCs were indeed due to direct, monosynaptic glutamatergic inputs from BLA axons to L5 neurons, as 4-AP allows direct depolarization of presynaptic terminals to release neurotransmitter without action potential propagation (**Figure 4B**).

We then evaluated the plasticity rules associated with these excitatory inputs using a protocol similar to those employed by Bittner et al. (2017) and Caya-Bissonnette et al. (2023) (**Figure 4C**). Baseline EPSCs were measured under voltage clamp for 10 minutes using a paired pulse stimulation protocol. The BTSP induction involved a train of synaptic inputs (10 EPSPs at 20 Hz; pre) followed by a burst of backpropagating action potentials (bAPs) via a 300 ms current injection (post), with a 500 ms delay between pre- and post-stimulation, repeated five times.

Contrary to previous findings with electrical stimulation, we observed no significant LTP following the BTSP induction protocol (94.05% of baseline). The paired-pulse ratio (PPR) of EPSCs remained unchanged post-induction (**Figure 4D**).

Despite evidence supporting the ability of L5 pyramidal neurons to integrate pre- and postsynaptic cues, our results indicate that amygdalar inputs to these neurons do not follow the same plasticity rules observed in other pathways.

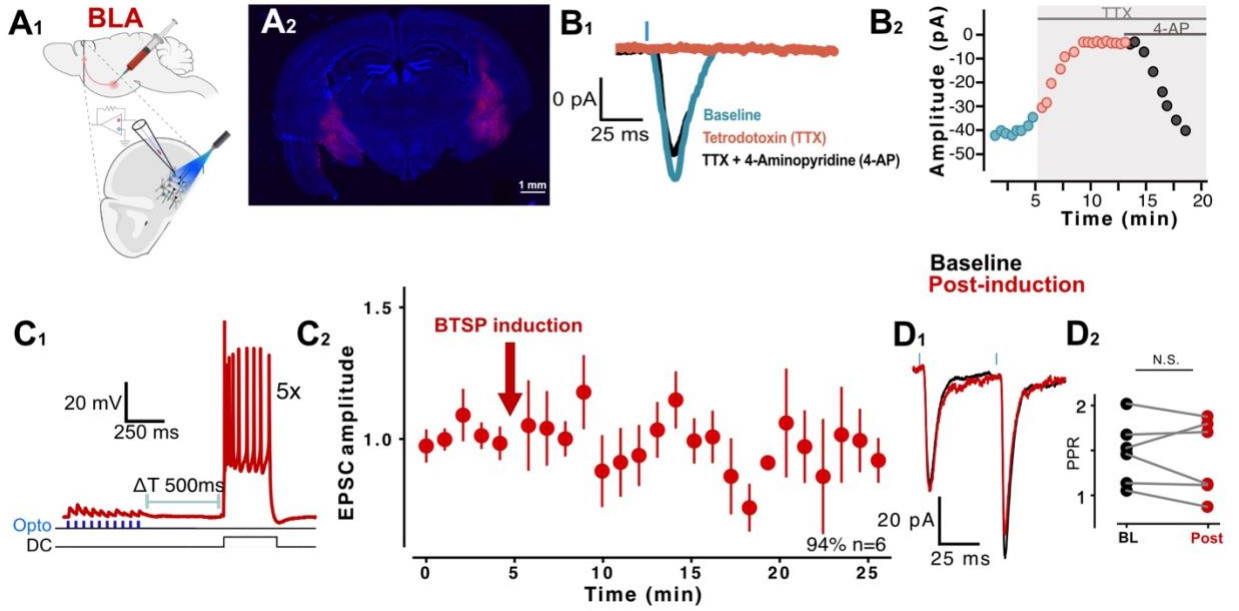

Figure 4. BLA inputs onto mPFC L5 neurons do not undergo BTSP. A) Schematic showing AAV-ChR2 injection followed by optogenetic stimulation and whole-cell electrophysiology. **B_1)** TTX was applied to block all synaptic transmissions, followed by the application of 4-AP to selectively restore the currents from monosynaptic inputs. The trace shown in teal is baseline EPSC in response to LED stimulation. Orange trace is following TTX application. Black trace shows restoration of presynaptic release following 4-AP addition. **B_2)** Quantification of EPSC amplitudes. Response was reduced upon TTX application, indicating the cessation of synaptic transmission. Subsequent application of 4-AP resulted in the recovery of EPSC amplitudes, confirming the restoration of currents specifically from monosynaptic inputs. **C_1)** BTSP induction protocol. 10 LED pulses are given at a frequency of 20 Hz, followed by bAPs (600 pA for 300 ms). The pairing protocol is repeated 5 times and the temporal delay between pre and post is ΔT= 500 ms. **C_2)** Normalized change in EPSC amplitude over time (n=6; 94.05% of baseline). **D_1)** Paired pulse EPSCs of baseline and post-BTSP induction traces. **D_2)** PPR of baseline traces (blue) and post-induction (magenta).

4.2 Commissural inputs onto mPFC L5 neurons do not undergo BTSP

To begin characterizing commissural inputs onto layer 5 pyramidal neurons in the medial prefrontal cortex (mPFC), we evaluated the role of AMPA receptors in mediating synaptic responses. This involved the application of NBQX, a selective antagonist of AMPA receptors. The administration of NBQX completely abolished EPSCs thereby confirming that these synaptic responses are indeed mediated by AMPA receptors (**Figure 5B**).

Next, we evaluated BTSP induction in this pathway. ChR2 was delivered via AAV only to the right hemisphere, enabling specific stimulation of axon terminals projecting to the opposite side. We employed the established BTSP induction protocol, consisting of 10 light-induced EPSPs at 20 Hz followed by a 300 ms current injection, with a 500 ms interval between pre- and post-stimulation (**Figure 5**). Similar to our findings with BLA inputs, the paired-pulse ratio (PPR) remained unchanged before and after the induction protocol.

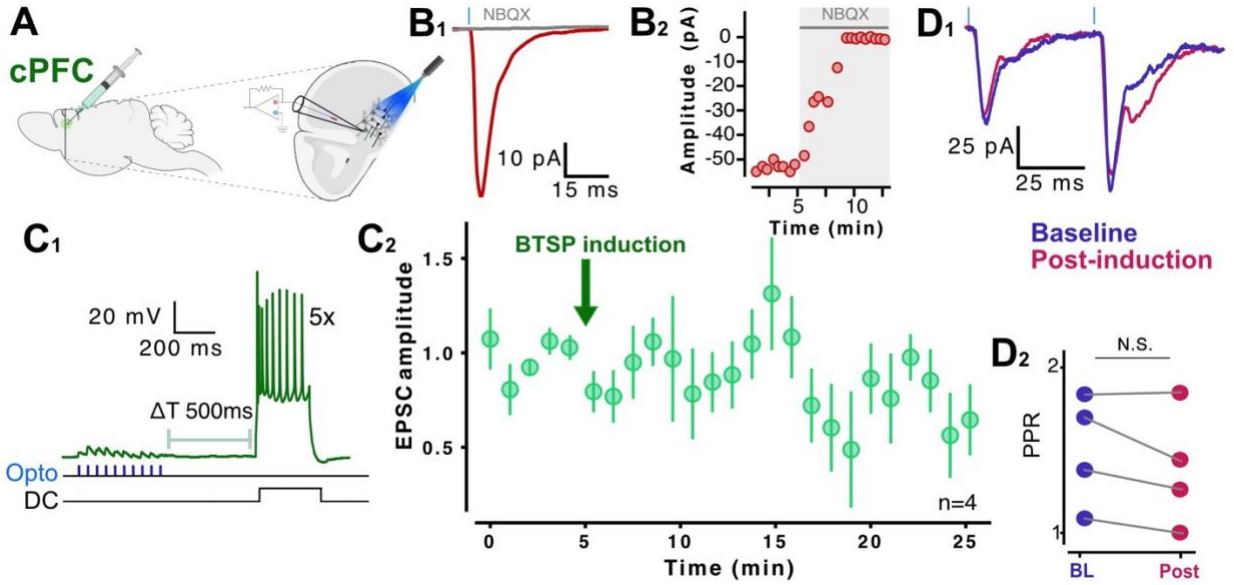

Figure 5. Commissural inputs onto mPFC L5 neurons do not undergo BTSP. A) Schematic showing AAV-ChR2 injection followed by optogenetic stimulation and whole-cell electrophysiology. **B_1)** EPSC traces before (red) and after (grey) the addition of NBQX to confirm AMPA receptor-mediated transmission. **B_2)** Quantification of the EPSC amplitudes shown in B_1. **C_1)** BTSP induction protocol. 10 LED pulses are given at a frequency of 20 Hz, followed by bAPs (600 pA for 300 ms). The pairing protocol is repeated five times and the temporal delay between pre and post is ΔT= 500 ms. **C_2)** Normalized change in EPSC amplitude over time (n=5; 95.04% of baseline). **D_1)** Paired

pulse EPSCs of baseline and post-BTSP induction traces. **D_2)** PPR of baseline traces (blue) and post-induction (magenta).

4.3 Hippocampal inputs onto mPFC L5 neurons undergo BTSP, with one shot induction

We first established baseline synaptic transmission characteristics. Using optogenetic activation, we triggered monosynaptic ChR2-induced EPSCs recorded from layer 5 pyramidal neurons. This baseline data confirmed the functional integrity and responsiveness of the synapses to controlled stimulation (**Figure 6A**). In exploring the vHIP-mPFC pathway, we modified the standard BTSP induction protocol to assess the impact of the number of action potentials on synaptic plasticity. Specifically, we injected 2500 pA of current for a 2 ms duration at 20 Hz, generating a total of 5 spikes, a notable adjustment from the typical 400-600 pA current injection for 300 ms used in previous experiments (**Figure 6C**).

We were also interested in seeing whether those inputs would undergo one-shot BTSP. That is, can vHIP synapses with L5 pyramidal neurons potentiate following one pairing of induction instead of 5? Surprisingly, this minimalistic induction protocol (one pairing vs five; and 5 postsynaptic spikes at 20 Hz vs 300 ms current injection) induced robust potentiation (**Figure 6**; 139.60% of baseline). Similar to previous findings, PPR did not change after BTSP induction. The ability of the vHIP-mPFC pathway to exhibit potentiation from just a single pairing highlights the unique synaptic characteristics of this connection, suggesting a capacity for rapid synaptic adjustments that may underpin one-shot learning.

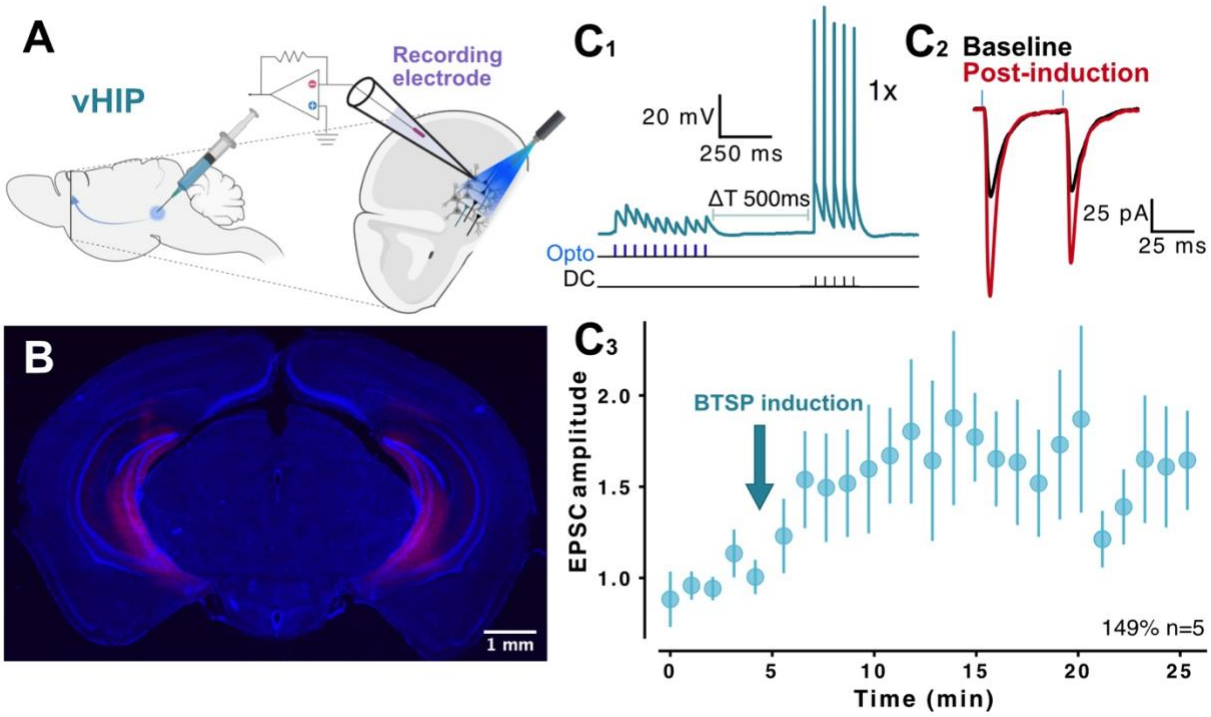

Figure 6. vHIP inputs onto mPFC L5 neurons undergo BTSP, *with one shot induction*. A) schematic showing general outline of optogenetic experiments. AAV-ChR2 is injected in the brain region of interest (ventral hippocampus; vHIP). Following a waiting period of 2-4 weeks for viral expression, whole-cell electrophysiology experiments are conducted. **B)** Hippocampal brain slice stained with DAPI. Injection site shown in red (mCherry). **C_1)** BTSP induction protocol. 10 LED pulses are given at a frequency of 20 Hz, followed by 5 postsynaptic spikes (2500 pA for 2 ms, 20 Hz). The pairing protocol is repeated once and the temporal delay between pre and post is ΔT= 500 ms. **C_2)** Paired pulse EPSCs of baseline and post-BTSP induction traces. **C_3)** Normalized change in EPSC amplitude over time (148.21% of baseline; n=5; p-value=0.0029).

4.4 Thalamic inputs onto mPFC L5 neurons undergo BTSP

We next examined long-range projections from the mediodorsal nucleus of the thalamus. Employing the standard BTSP protocol with 5 pairings and a 300 ms current injection, we observed a significant long-term potentiation (LTP) that was notably more robust than that induced by hippocampal inputs (179.29% of baseline, **Figure 7**).

Notably, the response of L5 neurons to LED-induced stimulation of thalamic terminals often exhibited polysynaptic activity, necessitating adjustments in our approach. Typically, only a single light pulse was used unless EPSCs were sufficiently clear to distinguish between sequential pulses.

When feasible, a paired pulse was administered, enabling a detailed assessment of synaptic dynamics. Consistent with results from other tested pathways, the paired-pulse ratio (PPR) remained stable, suggesting a postsynaptic locus of expression.

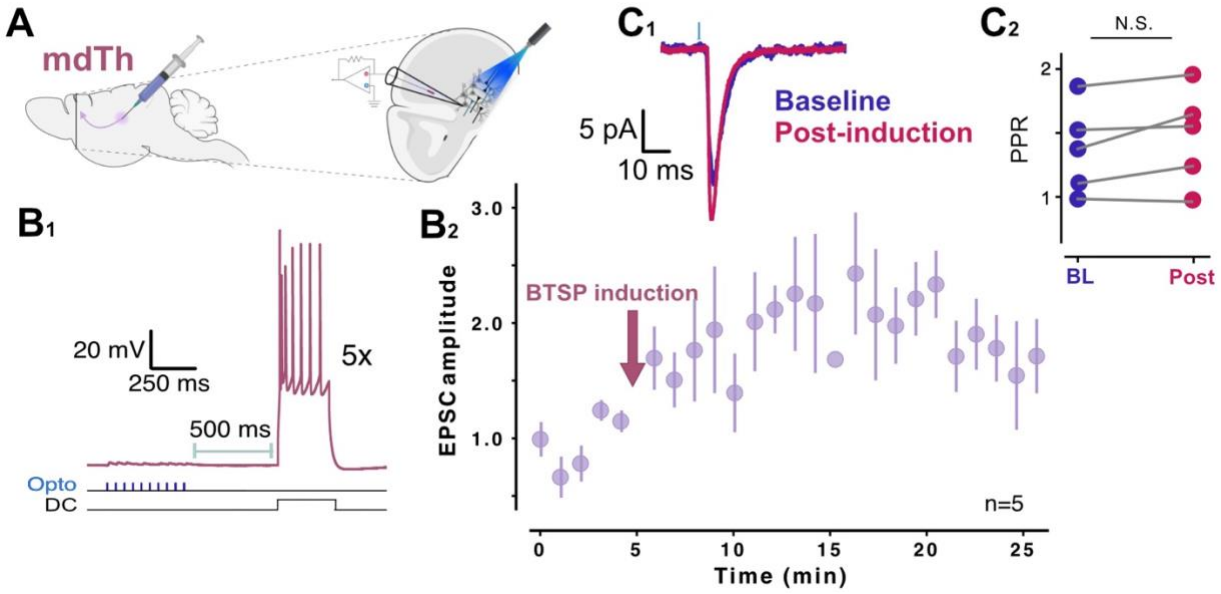

Figure 7. mdTh inputs onto mPFC L5 neurons undergo BTSP. A) Schematic showing AAV-ChR2 injection followed by optogenetic stimulation and whole-cell electrophysiology. **B_1)** BTSP induction protocol. 10 LED pulses are given at a frequency of 20 Hz, followed by bAPs (600 pA for 300 ms). The pairing protocol is repeated five times and the temporal delay between pre and post is ΔT= 500 ms. **B_2)** Normalized change in EPSC amplitude over time (n=5; 179.29% of baseline). **C_1)** EPSC of baseline and post-BTSP induction following LED stimulation (pulse width= 1 ms). **C_2)** PPR of baseline traces (blue) and post-induction (magenta).

4.5 BTSP induction protocol does not induce plasticity under physiological conditions

In our previous experiments, elevated Ca^{2+} concentrations (2.5 mM) were used in the artificial cerebrospinal fluid (ACSF). To explore BTSP under more physiological conditions, we conducted slice electrophysiology experiments with Ca^{2+} concentrations adjusted to biological levels (1.2, 1.5, and 1.8 mM).

4.5.1 Induction of BTSP at [Ca^{2+}] = 1.8 mM

In our first set of experiments within the physiological range, we tested the BTSP protocol at the highest calcium concentration ([Ca^{2+}] = 1.8 mM) used in the aCSF. Contrary to expectations

and previous results at [Ca^{2+}] = 2.5 mM, five pairings of our standard BTSP protocol—10 presynaptic stimulations at 20 Hz followed by backpropagating action potentials (bAPs, 600 pA for 300 ms or 500 ms) with a 500 ms delay—did not induce long-term potentiation (LTP) (113.06% of baseline; p-value=0.33; n=13; **Figure 8A**). Additionally, when we increased the number of protocol repetitions from 5 to 20, robust LTP was also observed (131% of baseline; p-value= 0.005; n=4; **Figure 8B**).

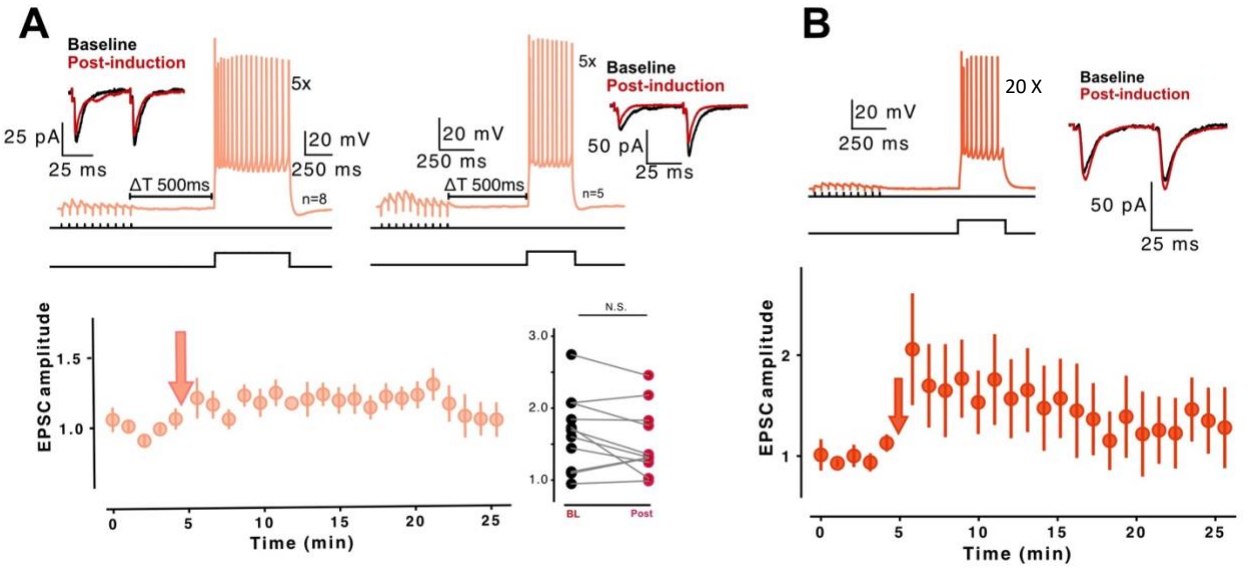

Figure 8. BTSP protocol does not induce plasticity under physiological conditions: [Ca^{2+}] = 1.8 mM. A) *Pairing 1:* pre: 10 synaptic inputs (20 Hz) and post (400-600 pA for 500 ms) with a temporal delay of ΔT= 500 ms. Protocol is repeated 5 times. Representative trace of baseline (black) and post-induction (red) EPSCs is shown (top left). *Pairing 2:* pre: 10 synaptic inputs (20 Hz) and post (400-600 pA for 300 ms) with a temporal delay of ΔT= 500 ms. Protocol is repeated 5 times. Representative trace of baseline (black) and post-induction (red) EPSCs is shown (top right). Plot of PPR is shown for all cells. Bottom plot shows Normalized EPSC change of both protocols shown in top panel. Arrow represents time of BTSP induction (113.06% of baseline; p-value=0.33; n=13). **B)** Pairing of pre: 10 synaptic inputs (20 Hz) and post (400-600 pA for 300 ms) with a temporal delay of ΔT= 500 ms. Protocol is repeated 20 times. Bottom plot shows Normalized EPSC change of both protocols shown in top panel. Arrow represents time of BTSP induction (131% of baseline; p-value= 0.005; n=4). Representative trace of baseline (black) and post-induction (red) EPSCs is shown (top right)

4.5.2 Induction of BTSP at [Ca^{2+}] = 1.5 mM

Further investigating the role of physiological calcium concentrations, we examined the effects at [Ca^{2+}] = 1.5 mM. Employing our standard protocol, we induced a train of 10 presynaptic stimulations at 20 Hz, followed by a burst of 10 action potentials (APs) delivered at 100 Hz (2500 pA current injection for 2 ms), with a 500 ms delay (ΔT). This arrangement did not result in any significant change in EPSC amplitude (118.16% of baseline; p-value= 0.17; n=5)

Lastly, we examined whether pairing the 15 stimulations (50 Hz) with bAPs (600 pA of current injection for 300 ms) for 10 times instead of 5 would have an effect. Indeed, following this pairing protocol, we observed stronger LTP (143.31% of baseline; p-value= 0.03; n=3; **Figure 9**).

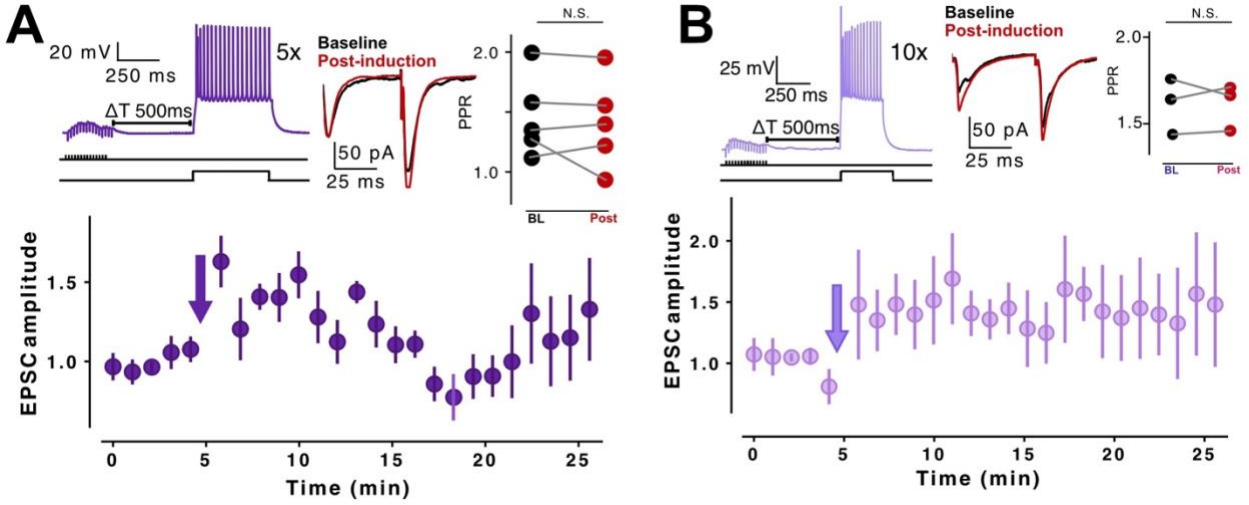

Figure 9. BTSP protocol does not induce plasticity under physiological conditions: [Ca^{2+}] = 1.5 mM. A) Pairing of pre: 15 synaptic inputs (50 Hz) and post (400-600 pA for 500 ms) with a temporal delay of ΔT= 500 ms. Protocol is repeated 5 times. Representative trace of baseline (black) and post-induction (red) EPSCs is shown. Plot of PPR is shown for all cells. Bottom plot shows Normalized EPSC change (118.16% of baseline; p-value= 0.17; n=5). Arrow represents time of BTSP induction. **B)** Pairing of pre: 15 synaptic inputs (50 Hz) and post (400-600 pA for 300 ms) with a temporal delay of ΔT= 500 ms. Protocol is repeated 10 times. Representative trace of baseline (black) and post-induction (red) EPSCs is shown (143.31% of baseline; p-value= 0.03; n=3). Plot of PPR is shown for all cells.

4.5.3 Induction of BTSP at [Ca^{2+}] = 1.2 mM

In the lowest [Ca^{2+}], we started by slightly modifying the BTSP protocol. Following the 10 synaptic inputs, we gave 5 (20 Hz; n=6; **Figure 10C**) or 10 (100 Hz; n=8; **Figure 10A**) postsynaptic spikes, using the same temporal delay of ΔT= 500 ms. This reversed the previously observed LTD to mild LTP (5 spikes: 130.75% of baseline, p-value= 0.0167; 10 spikes: 126% of baseline; p-value= 0.00268).

We examined whether reversing the order of pre- and post- stimulations within the standard BTSP protocol would show any modifications in lower calcium concentrations. We found that following 5 pairings of post-pre, mild LTP was produced (127% of baseline; p-value= 0.038; n=4; **Figure 10B**)

Next, we assessed the potential for one shot learning, using a protocol that consisted of a train of synaptic inputs (10 stimulations at 20 Hz) followed by 500 ms with either 5 (n=8) or 10 (n=3) postsynaptic spikes (2500 pA current injection for 2 ms). Contrary to expectations, this protocol elicited mild Long-Term Depression (LTD) rather than potentiation (84.62% of baseline; p-value= 0.045; n=11; **Figure 10D**).

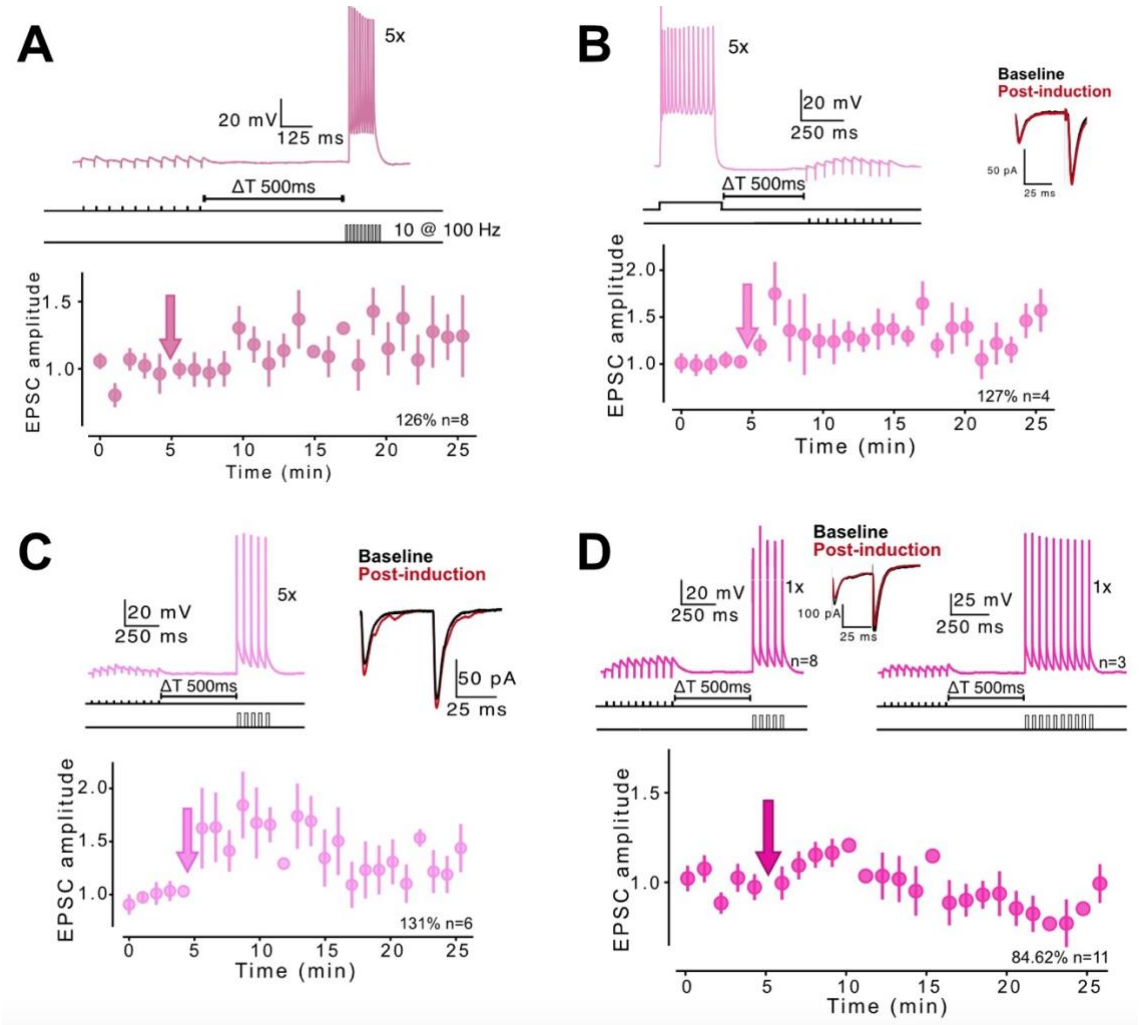

Figure 10. BTSP protocol does not induce plasticity under physiological conditions: [Ca^{2+}] =1.2 mM. A) Pairing of pre: 10 synaptic inputs (20 Hz) and post:10 postsynaptic spikes (100 Hz), with a temporal delay ΔT= 500 ms. Protocol was repeated 5 times. Normalized EPSC change shown in the plot at the bottom (126.00% of baseline; p-value= 0.000268; n=8). **B)** Pairing of post: bAPs (400-600 pA for 300 ms) and pre: 10 synaptic inputs (20 Hz), with a temporal delay ΔT= 500 ms. Protocol was repeated 5 times. Normalized EPSC change shown in the plot at the bottom (127% of baseline; p-value= 0.038; n=4). **C)** Pairing of pre: 10 synaptic inputs (20 Hz) and post: 5 postsynaptic spikes (20 Hz), with a temporal delay of ΔT= 500 ms. Protocol was repeated 5 times. Normalized EPSC change shown in the plot at the bottom (131% of baseline; p-value= 0.0167; n=6. **D)** One shot btsp induction. Left: pairing of pre: 10 synaptic inputs (20 Hz) and post: 5 spikes (20 Hz), with a delay of ΔT= 500 ms. Right: 10 synaptic inputs (20 Hz) and post: 10 spikes (20 Hz) with a delay of ΔT= 500 ms. Normalized EPSC change shown in the plot at the bottom (both protocols grouped; 84.62% of baseline; n=11). All arrows indicate time of BTSP induction. All paired pulse traces show baseline (black) and post-induction (red) EPSCs.

4.6 BTSP induction with a Hebbian eligibility trace leads to potentiation under physiological conditions

All previous BTSP induction protocols employed a train of 10 synaptic inputs (EPSPs) followed by an instructive signal (bAPs or individual postsynaptic spikes) with a temporal delay of ΔT= 500 ms. Care was taken to ensure that EPSPs did not trigger spiking during the pre-train phase. In our subsequent experiments, we aimed to investigate whether postsynaptic spiking during the train would influence the magnitude of the observed LTP. Initially, we used a high physiological concentration of calcium ($[Ca^{2+}]$ = 1.8 mM). When postsynaptic cells were allowed to spike during the EPSP train, we observed robust LTP, with an increase to 176.56% of baseline after 5 rounds of pairing (p-value = 0.0007; n=8; **Figure 11A**).

We extended this investigation to the lower end of the physiological calcium range ($[Ca^{2+}]$ = 1.2 mM). Similar to higher calcium levels, postsynaptic spiking during the presynaptic train led to a significant increase in EPSC amplitude (172.27% of baseline; p-value=1.04 x 10^{-5}; n=8; **Figure 11B**) after 5 repetitions. Intriguingly, this LTP was bidirectional; when postsynaptic backpropagating action potentials (bAPs) preceded the synaptic inputs by 500 ms, robust LTP was also achieved (151.76% of baseline; p-value=0.017; n=5; **Figure 11C**). Consistent with earlier findings, the paired-pulse ratio (PPR) remained unchanged.

To further explore this bidirectional plasticity, we reduced the number of pairings to one, assessing the potential for one-shot plasticity. Our results show no significant change in plasticity (94.94% of baseline; p-value=0.34; n=4; **Figure 11D**).

Building on these findings, we considered the work of Caya-Bissonnette et al. (2023), which revealed an absence of plasticity at intermediate timescales (ΔT=250 ms). Our next steps involved evaluating whether similar outcomes occur when the postsynaptic cell spikes during the *pre* train in the protocol. Interestingly, even though we observed more robust LTP at ΔT=500 ms with spiking during the synaptic train, reducing the ΔT to 250 ms abolished the LTP regardless of the order (pre-post: 97% of baseline, p-value= 0.45, n=4, **Figure 12A**; post-pre: 93% of baseline, p-value 0.14, n=5, **Figure 12C**), consistent with findings observed by Caya-Bissonnette *et al.* (2023).

We further reduced the temporal window to 0 ms (ΔT=0 ms) to determine whether the absence of plasticity is exclusive to intermediate timescales. During the pre-post protocol (5X), the average EPSC amplitude did increase from baseline, but the change is not significant (111.19% of baseline, p-value=0.16, n=5, **Figure 12B**). Interestingly, this protocol did not display the same bidirectionality observed with the other protocols at ΔT=500 ms and 250 ms. When we reversed the order to post-pre, we observed dramatic increase in EPSC amplitude relative to baseline, though not as robust as that observed at ΔT= 500 ms (138% of baseline, p-value=6.07×10^{-5}, n=6, **Figure 12D**).

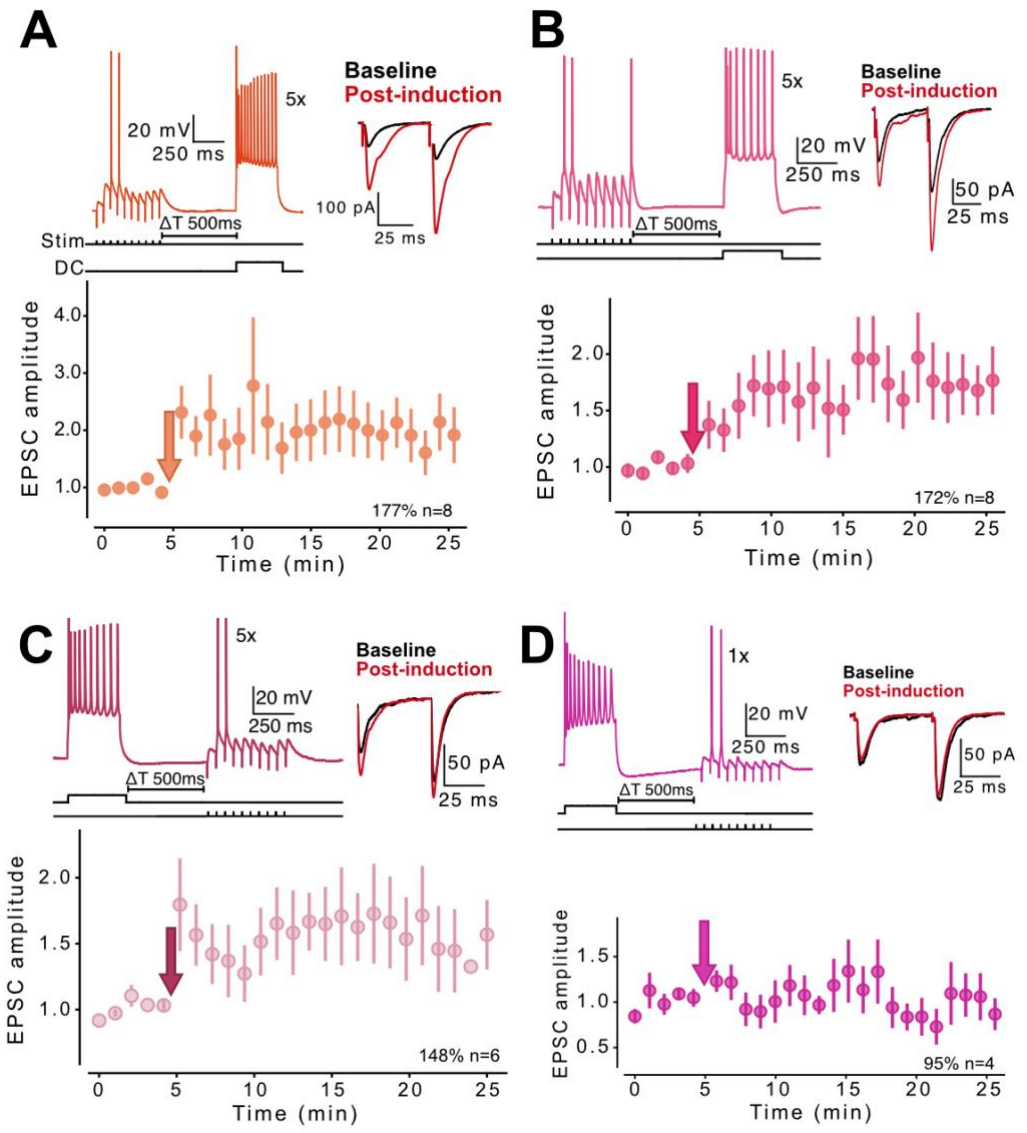

Figure 11. BTSP induction with a Hebbian eligibility trace at ΔT= 500 ms. A) Pairing of pre: 10 synaptic inputs (leading to postsynaptic spiking; 20 Hz) and post (400-600 pA for 300 ms) at a temporal delay of ΔT= 500 ms. Protocol is repeated 5 times. Representative trace of baseline (black) and post-induction (red) EPSCs is shown (top right). Normalized EPSC change shown in the plot at the bottom (176.56% of baseline; p-value= 0.0007; n=8). Experiment done at $[Ca^{2+}]$ = 1.8 mM. **B)** Same protocol as that shown in A. Experiment done at $[Ca^{2+}]$ = 1.2 mM. (172.27% of baseline; p-value=1.04 x 10-5; n=8). **C)** Pairing of post (400-600 pA for 300 ms) and pre (10 synaptic inputs leading to postsynaptic spikes; 20 Hz) at a temporal delay of ΔT= 500 ms. Protocol is repeated 5 times. Representative trace of baseline (black) and post-induction (red) EPSCs is shown (top right). Normalized EPSC change shown in the plot at the bottom (148.39% of baseline; p-value= 0.0052; n=6). Experiment conducted at $[Ca^{2+}]$ = 1.2 mM. **D)** Same protocol as that shown in C; with one pairing instead of 5. Experiment done at $[Ca^{2+}]$ = 1.2 mM. Arrows represent the time of BTSP induction (94.94% of baseline; p-value= 0.34; n=4).

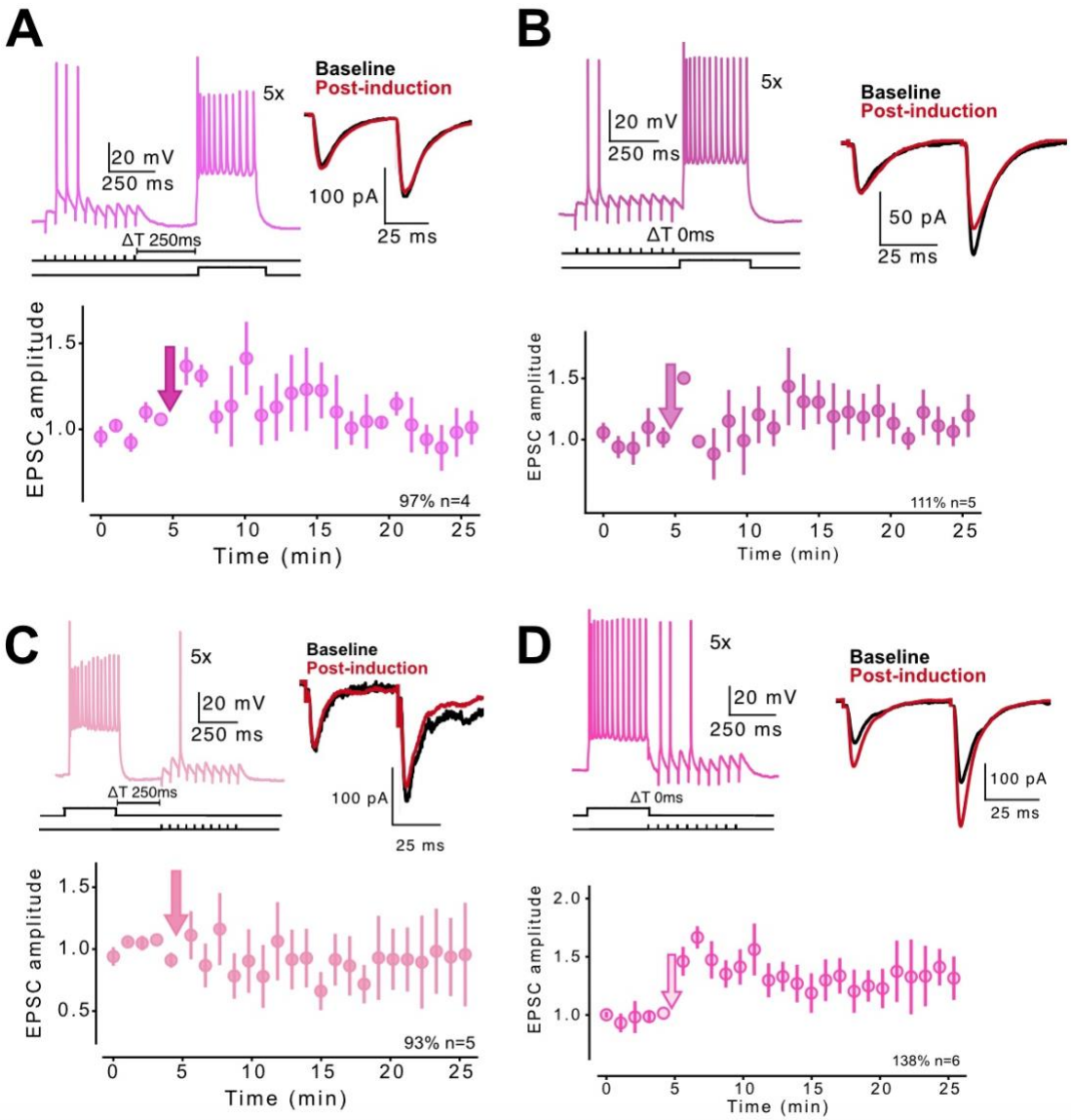

Figure 12. BTSP induction with a Hebbian eligibility trace at [Ca^{2+}] = 1.2 mM. A) Pairing of pre (10 synaptic inputs leading to postsynaptic spikes; 20 Hz) and post (400-600 pA for 300 ms) at a temporal delay of ΔT= 250 ms. Protocol is repeated five times. Representative trace of baseline (black) and post-induction (red) EPSCs is shown (top right). Normalized EPSC change shown in the plot at the bottom (97.13% of baseline; p-value= 0.45; n=4). **B)** Same protocol as that shown in A but with no temporal delay (ΔT= 0 ms). (111.19% of baseline; p-value= 0.16; n=5). **C)** Pairing of post (400-600 pA for 300 ms) and pre (10 synaptic inputs leading to postsynaptic spikes; 20 Hz) at a temporal delay of ΔT= 250 ms. Protocol is repeated 5 times. Representative trace of baseline (black) and post-induction (red) EPSCs is shown (top right). Normalized EPSC change shown in the plot at the bottom (93.10% of baseline; p-value= 0.14; n=5). **D)** Same protocol as that shown in C but with no temporal delay (ΔT= 0 ms). 137.50% of baseline; p-value= 6.07×10^{-5}; n=6. Arrows represent the time of BTSP induction.

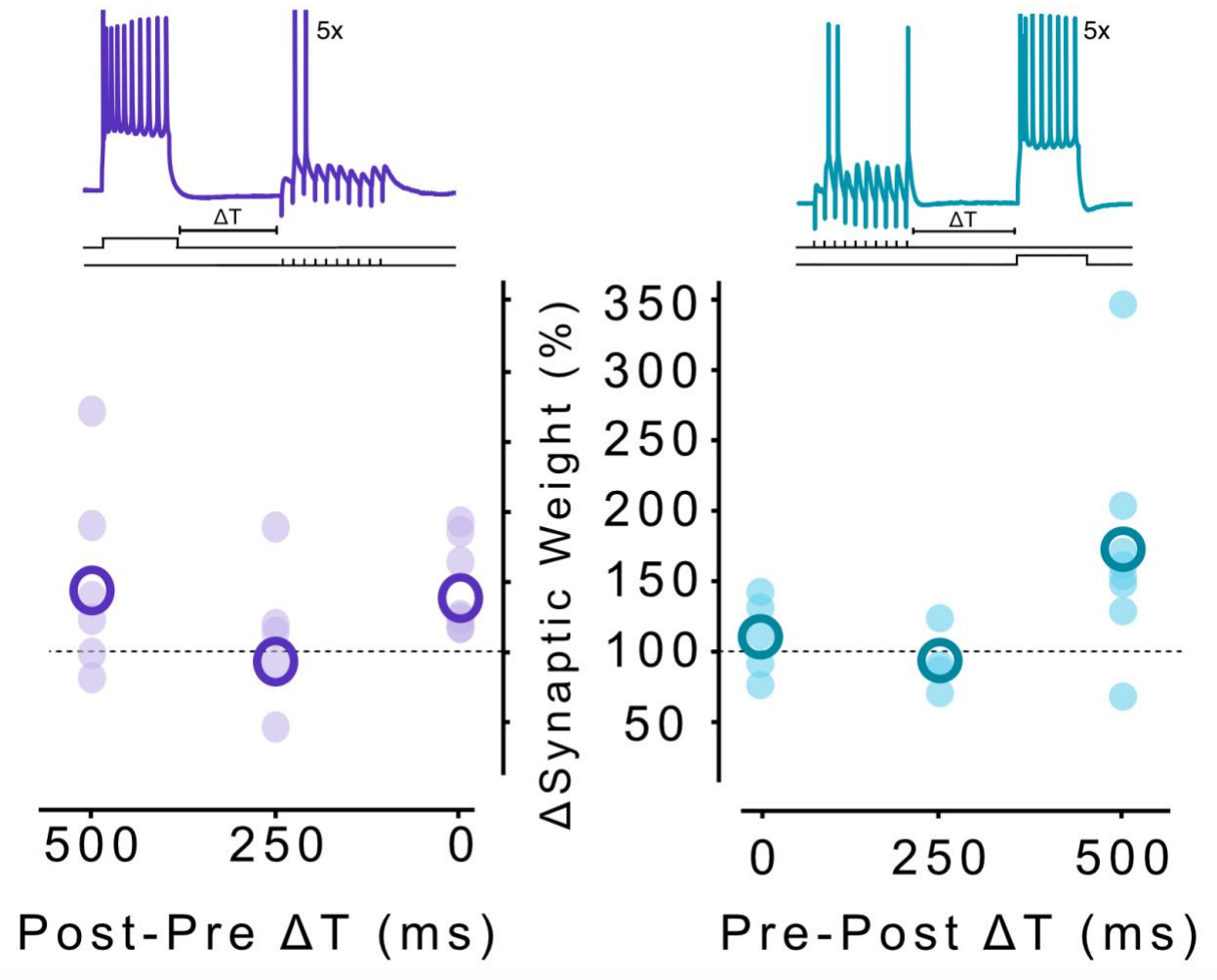

Figure 13. Resulting normalized changes in synaptic weight at different temporal delays. Left: Resulting mean synaptic weight change induced at different timing intervals from 0 ms to 500 ms for the *post-pre* order of BTSP induction (0 ms= 137.50%; 250 ms= 93.10%; 500 ms= 148%). **Right:** Resulting mean synaptic weight change induced at different timing intervals from 0 ms to 500 ms for the *pre-post* order of BTSP induction (0 ms= 111%; 250 ms= 97%; 500 ms= 172%).

5. Discussion

Exploring the neural mechanisms that underlie learning and memory represents a fundamental quest in neuroscience. Central to this inquiry is the question of why we learn. To delve into this question, it is essential to first define learning. In the context of this work, learning is defined as the acquisition of neuronal representations of new information, which can be stored

in short or long-term memory, thereby influencing our decisions and behaviors. From an evolutionary perspective, learning plays a crucial role in enabling organisms to adapt to their environments, acquire new skills, and enhance survival prospects. Despite the pivotal role of learning in shaping our everyday experiences, the precise cellular mechanisms underlying this process remain to be fully elucidated

Synaptic plasticity has long been proposed as a key mechanism underlying learning and memory formation. However, the current cellular model of STDP falls short in addressing fundamental features of associative learning at the behavioral level. This Hebbian form of plasticity necessitates the activation of pre- and postsynaptic neurons within a narrow time window of less than 50 ms, which contrasts with the broader time window separating behavioral associations. Additionally, the number of repetitions required to induce LTP is considerably higher than what is typically observed during associative learning tasks. For example, consider a gamer who learns to associate hearing a specific sound cue in a video game with imminent danger or an opportunity to gain points. It takes only a few rounds for them to adapt their behavior upon hearing this tone again. In this case, the time window between the tone and the outcome is at least a few hundred milliseconds long (200 ms – 2 s). This simple association deviates from the rules dictated by STDP protocols.

Recent research by Caya-Bissonnette et al. (2023) has tackled these challenges using a diverse array of experimental techniques, including whole-cell recordings of L5 PFC neurons, two-photon BTSP in the mouse prefrontal cortex, addressing the temporal delay and repetition frequency issues previously unaccounted for in the STDP model.

The mouse PFC serves as a convergence point for inputs from many brain regions, including the amygdala, thalamus, hippocampus, and the contralateral side of the PFC. Each of these pathways relays distinct types of information to the cortex, potentially leading to different plasticity rules within these circuits. For instance, inputs from the amygdala are known for their involvement in emotional processing; thalamic inputs play a role in working memory; the hippocampal inputs provide the cortex with contextual updates of the animal's state; and inputs from the contralateral side contribute to cognitive functions such as executive control and

decision-making, potentially involving plasticity mechanisms linked to cognitive flexibility and adaptation.

Previous cell electrophysiology experiments by Caya-Bissonnette *et al.* (2023) relied on electrical stimulation that activated synapses of unknown identity. This approach limited the ability to discern specific synaptic connections undergoing BTSP. To address this, we focused on elucidating which synaptic pathways arriving to the PFC undergo BTSP. By employing optogenetic techniques to study each pathway in isolation, we were able to determine that only two out of the four inputs tested display the same plasticity rules previously reported by Caya-Bissonnette *et al.* (2023). This discussion delves into the significance of these findings, attempts to explore the factors contributing to the differential plasticity observed among the tested synaptic inputs, and proposes avenues for future experimental work to build upon and expand our understanding of synaptic plasticity mechanisms in the PFC.

5.1 BTSP rules of different inputs arriving to the PFC

We tested inputs arriving from four different brain regions and making synapses with L5 pyramidal neurons in the mouse PFC: the basolateral amygdala (BLA), the ventral hippocampus (vHIP), the mediodorsal thalamus (mdTh), and inputs arriving from the other hemisphere (cPFC). Our initial hypothesis was that these inputs, despite relaying different information to the PFC, will exhibit similar plasticity rules since this form of BTSP is thought to have a postsynaptic locus of expression. This is further confirmed by the fact that PPR did not change between baseline and post-induction protocols. PPR is a measure of short-term plasticity dynamics that reflect changes in neurotransmitter release probability. A decrease in PPR reflects an increase in release probability and vice versa. Thus, the relatively constant PPR observed in these experiments suggests that the observed effects are more likely to be mediated by postsynaptic modifications.

Surprisingly, only projections from the vHIP and mdTh showed similar BTSP profiles to those documented by Caya-Bissonnette et al (2023). It is worth noting that both vHIP and mdTh preferentially contact L5 neurons in the PL region, whereas the BLA and cPFC are more likely to synapse onto those cells in the IL cortex. The two divisions of the PFC have been proposed to

underlie different, often opposing roles at the behavioral level, and thus might integrate information in such a way that accounts for the different plasticity rules seen in the results presented here.

In order to determine whether the inputs under study make monosynaptic connections to L5 pyramidal neurons, we utilized TTX and 4-AP in our optogenetic approaches. TTX is a Na^+ channel blocker, preventing the propagation of action potentials along the axon, which then ultimately blocks polysynaptic activity. Bath application of TTX completely abolished optogenetically evoked EPSCs. This means that AP firing and propagation down the BLA axons is required. It also indicates that light stimulation is insufficient to induce neurotransmitter release from ChR2-expressing axons. 4-AP blocks K^+ channels and thus increases depolarization, making direct depolarization by ChR2 sufficient to trigger glutamate release even in the presence of TTX.

Overall, our results show that all four inputs tested make monosynaptic connections with L5 pyramidal neurons in the mouse prefrontal cortex. Of those four pathways, only projections arriving from the ventral hippocampus and the mediodorsal thalamus can bind temporally separated signals in a manner consistent with BTSP rules. This suggests that there are pathway specific plasticity rules unique to vHIP-mPFC and mdTh-mPFC connections, indicating their capacity to integrate inputs separated by behavioral timescales.

One avenue for subsequent investigation entails exploring the potential instructive role of non-plastic pathways following BTSP induction, such as the BLA-mPFC and cPFC-mPFC connections. Rather than being eligible for potentiation according to BTSP rules, these pathways could serve as instructive signals, allowing other pathways to undergo plasticity upon the delayed instructive cue. Moreover, considering that the remaining two pathways are implicated in relaying information related to memory, including spatial (vHIP) and short-term (mdTh) working memory, future studies could shed light on how plasticity profiles differ in pathological contexts. For instance, investigating synaptic plasticity dynamics in mouse models of Alzheimer's disease, which fundamentally affects memory function, may offer valuable insights into the underlying mechanisms of memory impairment in dementia contexts.

5.2 BTSP under physiological conditions

The experimental conditions utilized to investigate the aforementioned inputs involved the use of elevated concentrations of Ca^{2+} (2.5 mM) in the artificial cerebrospinal fluid (ACSF). Such elevated concentrations are conventionally employed due to their experimental feasibility and their ability to enhance neurotransmitter release and facilitate synaptic transmission, which are essential considerations when studying novel inputs. However, this practice raises concerns regarding the reliability of the results obtained and their correlation with the mechanisms underlying learning at the behavioral level.

To address this concern, we conducted BTSP slice electrophysiology experiments under varying Ca^{2+} concentrations within the physiological range (1.2, 1.5, and 1.8 mM), in parallel with the optogenetic experiments. Due to the considerable time and resources involved in optogenetic experiments, which necessitated surgery, a waiting period of two to four weeks post-surgery, and subsequent electrophysiological recordings, we decided to not incorporate the physiological calcium experiments directly into the optogenetic protocol. Instead, we focused on establishing physiological BTSP rules using control mice, which can serve as a robust foundation for subsequent optogenetic investigations. This approach not only provides insights into how calcium dynamics influence synaptic function and plasticity but also lays the groundwork for establishing a physiological BTSP protocol to be utilized in optogenetic experiments to investigate synapse specific plasticity rules.

When conducting experiments under the lowest [Ca^{2+}] within the physiological range (1.2 mM), we found that without postsynaptic spiking during the synaptic train stimulations, BTSP experiments show no change in synaptic weight, which was observed at higher calcium concentrations. Interestingly, this novel protocol with a "Hebbian eligibility trace" follows similar temporal profile to that observed by Caya-Bissonnette *et al. (2023)*. That is, at intermediate timescales (ΔT=250 ms), we observed a lack of plasticity. Interestingly, this observation was bidirectional. We then shortened the temporal delay to ΔT= 0 ms. The post-pre order revealed potentiation, similar to findings by Caya-Bissonnette *et al.* (2023), and unlike the extended and intermediate temporal delays, this plasticity was not bidirectional at short timescales.

In conclusion, this work has provided significant insights into the synaptic mechanisms that underpin learning and memory, particularly through the lens of Behavioral Timescale Synaptic Plasticity (BTSP). By employing optogenetic techniques, we have isolated and analyzed synaptic inputs from various brain regions to layer 5 pyramidal neurons in the mouse prefrontal cortex (PFC), uncovering distinct plasticity rules that are specific to the ventral hippocampus and the mediodorsal thalamus. These findings highlight the potential for BTSP to integrate neuronal signals over timeframes that align with behavioral experiences, thereby providing a more accurate model of how learning occurs in natural settings.

Moreover, our approach using optogenetics has profound implications for future behavioral studies, suggesting that manipulating these pathways could directly influence learning and memory outcomes, providing a powerful tool for exploring the functional significance of synaptic connections in cognitive processes.

As we move forward, it is essential to integrate these findings with behavioral models to further elucidate the functional relevance of BTSP in learning and memory. Exploring these synaptic mechanisms in pathological models, such as Alzheimer's disease, could also reveal how disruptions in BTSP may contribute to the cognitive deficits observed in such conditions, offering new avenues for therapeutic interventions. Ultimately, this thesis not only advances our understanding of the synaptic basis of learning but also sets the stage for future research that bridges the gap between cellular mechanisms and behavioral outcomes.

6. Methodology

6.1 Slice Preparation

Male and Female C57BL/6 P20-P35 mice were used for slice electrophysiology experiments in accordance with procedures approved by the University of Ottawa Animal Care and Veterinary Services. Mice were anesthetized by inhalation of isoflurane (Baxter Corporation) before being euthanized by decapitation. The mouse brain was immediately removed into ice-cold Choline dissection buffer containing (in mM): 119.0 choline chloride, 2.5 KCl, 4.3 $MgSO_4$, 1.0 $CaCl_2$, 1.0

NaH2PO4, 1.3 Na ascorbate, 11.0 glucose, 26.2 NaHCO3 saturated with 95% O2/5% CO2 (pH =7.3; 295-300 mOsm/L). For optogenetic experiments, or electrical stimulation experiments with older mice (>P35), NMDG solution was used for transcardial perfusion in accordance with the protocol discussed by Ting et al., (2018). A Leica VT1000S vibratome was used to obtain 300 µm sections of the PFC in the choline (or NMDG solution). After sectioning, slices were transferred to a recovery chamber containing artificial cerebrospinal fluid (aCSF) containing (in mM): 119 NaCl, 2.5 CaCl2*, 1.3 MgSO4-7H2O, 1 NaH2PO4, 26.2 NaHCO3, and 11 glucose, at a temperature of 34 ℃ bubbled with 95% O2, 5 CO2. *Note CaCl2 concentration listed here only applies to optogenetic experiments; 0.9 mM MgSO4-7H2O and 1.2, 1.5, and 1.8 mM CaCl2 concentrations were also used to study BTSP under more physiological settings. NaCl was added to the aCSF to reach 295-300 mOsm when lower [CaCl2] and [MgSO4-7H2O] are used.

6.1.1 Solutions

Before obtaining acute brain slices, the following solutions will be prepared and stored for up to 1 week before recording:

- High [Ca^{2+}] ACSF solution, (in mM): 119.0 NaCl, 2.5 KCl, 1.3 MgSO4-7H2O, 2.5 CaCl2-2H2O, 1.0 NaH2PO4, 26.0 NaHCO3, 11.0 Glucose. Water is added to obtain a final osmolality (osm) of 295-300mmol/kg.
- Low [Ca^{2+}] ACSF solution, (in mM): 119.0 NaCl, 2.5 KCl, 1.0 MgSO4-7H2O, [1.2, 1.5, or 1.8 mM CaCl2-2H2O], 1.0 NaH2PO4, 26.0 NaHCO3, 11.0 Glucose. NaCl is added to obtain a final osmolality (osm) of 295-300mmol/kg.
- NMDG solution: as described in Ting et al (2018).
- NMDG-HEPES solution: as described in Ting et al (2018).
- Internal solution: (in mM): 115 potassium gluconate, 20 KCl, 10 sodium phosphocreatine, 10 HEPES, 4 ATP(Mg^{2+}), and 0.5 GTP (pH adjusted with KOH). pH= 7.25 and osmolality of 280-290 mOsmol/L

6.2 Optogenetic viral injections

For Channelrhodopsin (ChR2) expression, 200nL of AAV-CAG-ChR2 (H134R)-WPRE-SV40-mCherry will be injected in the target brain region (i.e., vHIP, BLA, mdTh). Injection volume and rate= 200nL @ 33nl/min. Titer= 3.3E13. Mice were allowed to recover for at least 2-4 weeks before obtaining ex vivo recordings (Figure 3).

cBLA= AP: –1.7 mm; ML: –3.0; DV: –5.1

vHIP coordinates= AP: -3.0; ML: +/-3.3; DV: -3.6 and -4.2.

mdTh= AP: –1.5; ML: -/+ 0.4; DV: –3.2

cPFC= AP: +1.7; ML: 0.3; DV: -2.3

6.3 Whole-Cell Electrophysiology

PFC slices were placed in a recording chamber, heated at 30-32℃, and L5 pyramidal neurons were visualized under differential interference contrast (DIC) with 40X submersive objective. Borosilicate glass recording electrodes (4 – 6 MΩ) were pulled using a Narishige PC-10 pipette puller (Narishige, Japan), filled with potassium-gluconate (K-Gluc) internal solution (supplemented with picrotoxin (PTX; Abcam), a Gamma-aminobutyric acid (GABA-A) receptor blocker to isolate excitatory currents) will be used for obtaining whole cell recordings. Internal solution was prepared in advance and stored at -80℃ until the day of the experiment

Whole-cell recordings were performed using an Axon Multiclamp 700B amplifier; current and voltage were low-pass filtered at 2 kHz filter and sampled with an Axon Digidata 1440A at 10 kHz. Slices were constantly supplied with aCSF (of varying [Ca^{2+}], depending on the experiment). For optogenetic stimulation, light (465 nm) was delivered through Colibri.2 LED Light Source (Zeiss) applied to acute PFC slices through a 40× water-immersion objective. Light intensity and pulse width (1 – 5 ms) were adjusted accordingly to elicit measurable EPSCs.

Access resistance was monitored on each sweep using a 200 ms, 5 mV hyperpolarizing pulse, for voltage clamp recordings, or with a 400 ms, -25 pA current injection for current clamp recordings, each induced at least 800 ms prior to electrical synaptic stimulations. Recordings with

large Ra fluctuations (>30%) were not included in analysis. When performing experiments in current-clamp, small direct current injection was sometimes used to maintain the cell between -75 and -65 mV.

6.4 BTSP experiments

A stimulation electrode (4 – 6 MΩ) filled with Ringer was positioned proximal to L5 neurons in PFC slices. An iso-flex ULC stimulation box was used to control the stimulating electrode. electrical stimuli were 0.1 ms in duration (for some experiments, a longer duration of 0.2 – 0.3 ms was used to induce post-synaptic spiking during the pairing protocol, see section 3.6). The intensity of electrical stimulation was adjusted to obtain EPSCs of ~20 – 100 pA during baseline recordings. A paired pulse (ΔT= 50 ms) was given every 20 s for 10 minutes during baseline and 20 minutes for post-induction voltage-clamp recordings. Each minute on BTSP plots is an average of 3 time points (or less if some sweeps were polysynaptic, which were then deleted and not included for analysis). The BTSP induction protocol was carried out in current-clamp. The pairing protocol consist of 10 electrical stimulations (pre) at a frequency of 20 Hz (unless otherwise stated), followed by 400 pA – 600 pA of current injection for 300 ms (bAPs; post). The time delay between pre and post is usually 500 ms (unless otherwise stated; see section 3.6). For most experiments, this pre-post pairing was repeated 5 times every 15 seconds, except when testing for one-shot learning, where pairing was only repeated once.

For optogenetic experiments, viral injections were performed on P20-P35 mice. Following a waiting period of 2-4 weeks for viral expression, whole-cell electrophysiology experiments were done as explained above. Light pulses were used in lieu of electrical stimulation to activate ChR2-expressing axons.

6.5 Data Analysis

Recordings were stored and analyzed on Clampfit 10.7 (Molecular Devices) and python programming language (Numpy and Scipy libraries). n refers to the number of neurons recorded

per experimental protocol. All experiments were conducted on different cells. The first EPSC of the paired pulse was used to assess plasticity pre and post BTSP induction. All EPSC values were normalized to the last 5 minutes of baseline amplitudes. The mean change was calculated using baseline amplitudes and the last 5 minutes of post-induction recordings. The amplitude of the second pulse relative to the first in the paired pulse was used to calculate PPR for baseline and post-induction.

References

Abraham, W. C., & Williams, J. M. (2003). Properties and Mechanisms of LTP Maintenance. *SAGE Journals*, *9*(6), 463–474. https://doi.org/10.1177/1073858403259119

Anastasiades, P. G., & Carter, A. G. (2021). Circuit organization of the rodent medial prefrontal cortex. *Trends in Neurosciences*, *44*(7), 550–563. https://doi.org/10.1016/J.TINS.2021.03.006

Andersen, N., Krauth, N., & Nabavi, S. (2017). Hebbian plasticity in vivo: relevance and induction. *Current Opinion in Neurobiology*, *45*, 188–192. https://doi.org/10.1016/J.CONB.2017.06.001

Axmacher, N., Elger, C. E., & Fell, J. (2008). Ripples in the medial temporal lobe are relevant for human memory consolidation. *Brain*, *131*(7), 1806–1817. https://doi.org/10.1093/BRAIN/AWN103

Bain, A. (1855). Of sensation. *John W Parker & Son, West Strand*, 119–248. https://doi.org/10.1037/12115-004

Bain, A. (1872). *Mind and Body: The Theories of Their Relation*.

Barbas, H., & Blatt, G. J. (1995). Topographically specific hippocampal projections target functionally distinct prefrontal areas in the rhesus monkey. *Wiley Online LibraryH Barbas, GJ BlattHippocampus, 1995•Wiley Online Library*, *5*(6), 511–533. https://doi.org/10.1002/hipo.450050604

Bassi, M. S., Iezzi, E., Gilio, L., Centonze, D., & Buttari, F. (2019). Synaptic Plasticity Shapes Brain Connectivity: Implications for Network Topology. *International Journal of Molecular Sciences 2019, Vol. 20, Page 6193*, *20*(24), 6193. https://doi.org/10.3390/IJMS20246193

Bechara, A., Damasio, H., Damasio, A. R., & Lee, G. P. (1999). Different Contributions of the Human Amygdala and Ventromedial Prefrontal Cortex to Decision-Making. *Journal of Neuroscience*, *19*(13), 5473–5481. https://doi.org/10.1523/JNEUROSCI.19-13-05473.1999

Benetti, S., Mechelli, A., Picchioni, M., Broome, M., Williams, S., & McGuire, P. (2009). Functional integration between the posterior hippocampus and prefrontal cortex is impaired in both first episode schizophrenia and the at risk mental state. *Brain*, *132*(9), 2426–2436. https://doi.org/10.1093/BRAIN/AWP098

Bi, G. Q., & Poo, M. M. (1998). Synaptic Modifications in Cultured Hippocampal Neurons: Dependence on Spike Timing, Synaptic Strength, and Postsynaptic Cell Type. *Journal of Neuroscience*, *18*(24), 10464–10472. https://doi.org/10.1523/JNEUROSCI.18-24-10464.1998

Bittner, K. C., Milstein, A. D., Grienberger, C., Romani, S., & Magee, J. C. (2017). Behavioral time scale synaptic plasticity underlies CA1 place fields. *Science*, *357*(6355), 1033–1036. https://doi.org/10.1126/SCIENCE.AAN3846/SUPPL_FILE/AAN3846_BITTNER_SM.PDF

Bliss, T. V. P., Collingridge, G. L., Morris, R. G. M., & Reymann, K. G. (2018). Long-term potentiation in the hippocampus: Discovery, mechanisms and function. *Neuroforum*, *24*(3), A103–A120. https://doi.org/10.1515/NF-2017-A059/ASSET/GRAPHIC/J_NF-2017-A059_FIG_002.JPG

Bliss, T. V. P., & Lømo, T. (1973a). Long-lasting potentiation of synaptic transmission in the dentate area of the anaesthetized rabbit following stimulation of the perforant path. *The Journal of Physiology*, *232*(2), 331–356. https://doi.org/10.1113/JPHYSIOL.1973.SP010273

Bliss, T. V. P., & Lømo, T. (1973b). Long-lasting potentiation of synaptic transmission in the dentate area of the anaesthetized rabbit following stimulation of the perforant path. *The Journal of Physiology*, *232*(2), 331–356. https://doi.org/10.1113/JPHYSIOL.1973.SP010273

Bock, T., & Stuart, G. J. (2016). Impact of calcium-activated potassium channels on NMDA spikes in cortical layer 5 pyramidal neurons. *Journal of Neurophysiology*, *115*(3), 1740–1748. https://doi.org/10.1152/JN.01047.2015/ASSET/IMAGES/LARGE/Z9K0041635600004.JPEG

Bradfield, L. A., Hart, G., & Balleine, B. W. (2013). The role of the anterior, mediodorsal, and parafascicular thalamus in instrumental conditioning. *Frontiers in Systems Neuroscience*, *7*(OCT). https://doi.org/10.3389/FNSYS.2013.00051/FULL

Brockway, E. T., Simon, S., & Drew, M. R. (2023). Ventral hippocampal projections to infralimbic cortex and basolateral amygdala are differentially activated by contextual fear and extinction recall. *Neurobiology of Learning and Memory*, *205*, 107832. https://doi.org/10.1016/J.NLM.2023.107832

Brown, E. C., Clark, D. L., Hassel, S., MacQueen, G., & Ramasubbu, R. (2017). Thalamocortical connectivity in major depressive disorder. *Journal of Affective Disorders*, *217*, 125–131. https://doi.org/10.1016/J.JAD.2017.04.004

Burgos-Robles, A., Vidal-Gonzalez, I., & Quirk, G. J. (2009). Sustained Conditioned Responses in Prelimbic Prefrontal Neurons Are Correlated with Fear Expression and Extinction Failure. *Journal of Neuroscience*, *29*(26), 8474–8482. https://doi.org/10.1523/JNEUROSCI.0378-09.2009

Castellani, G. C., Quinlan, E. M., Cooper, L. N., & Shouval, H. Z. (2001). A biophysical model of bidirectional synaptic plasticity: Dependence on AMPA and NMDA receptors. *Proceedings of the National Academy of Sciences*, *98*(22), 12772–12777. https://doi.org/10.1073/PNAS.201404598

Caya-Bissonnette, L., Naud, R., & Béïque, J.-C. (2023). Cellular Substrate of Eligibility Traces. *BioRxiv*, 2023.06.29.547097. https://doi.org/10.1101/2023.06.29.547097

Chauveau, F., Célérier, A., Ognard, R., … C. P.-B. brain, & 2005, U. (2005). Effects of ibotenic acid lesions of the mediodorsal thalamus on memory: relationship with emotional processes in mice. *Behavioural Brain Research*, *156*(2), 215–223.

Citri, A., & Malenka, R. C. (2007). Synaptic Plasticity: Multiple Forms, Functions, and Mechanisms. *Neuropsychopharmacology 2008 33:1*, *33*(1), 18–41. https://doi.org/10.1038/sj.npp.1301559

Collingridge, G. L., Olsen, R. W., Peters, J., & Spedding, M. (2009). A nomenclature for ligand-gated ion channels. *Neuropharmacology*, *56*(1), 2–5. https://doi.org/10.1016/J.NEUROPHARM.2008.06.063

Collins, D. P., Anastasiades, P. G., Marlin, J. J., & Carter, A. G. (2018). Reciprocal Circuits Linking the Prefrontal Cortex with Dorsal and Ventral Thalamic Nuclei. *Neuron*, *98*(2), 366-379.e4. https://doi.org/10.1016/J.NEURON.2018.03.024

Debanne, D., Gähwiler, B. H., & Thompson, S. M. (1998). Long-term synaptic plasticity between pairs of individual CA3 pyramidal cells in rat hippocampal slice cultures. *The Journal of Physiology*, *507*(Pt 1), 237. https://doi.org/10.1111/J.1469-7793.1998.237BU.X

Dembrow, N. C., Chitwood, R. A., & Johnston, D. (2010). Projection-Specific Neuromodulation of Medial Prefrontal Cortex Neurons. *Journal of Neuroscience*, *30*(50), 16922–16937. https://doi.org/10.1523/JNEUROSCI.3644-10.2010

Dilgen, J., Tejeda, H. A., & O'Donnell, P. (2013). Amygdala inputs drive feedforward inhibition in the medial prefrontal cortex. *Journal of Neurophysiology*, *110*(1), 221–229. https://doi.org/10.1152/JN.00531.2012/ASSET/IMAGES/LARGE/Z9K0141319980007.JPEG

Dingledine, R., Borges, K., & Bowie, D. (1999). The glutamate receptor ion channels. *ASPET*.

Drew, P. J., & Abbott, L. F. (2006). Extending the effects of spike-timing-dependent plasticity to behavioral timescales. *Proceedings of the National Academy of Sciences*, *103*(23), 8876–8881. https://doi.org/10.1073/PNAS.0600676103

Dudchenko, P. A. (2004). An overview of the tasks used to test working memory in rodents. *Neuroscience & Biobehavioral Reviews*, *28*(7), 699–709. https://doi.org/10.1016/J.NEUBIOREV.2004.09.002

Dudek, S. M., & Bear, M. F. (1992). *Homosynaptic long-term depression in area CAl of hippocampus and effects of N-methyl-D-aspartate receptor blockade (long-term potentiation/hippocampal slice/synaptic plasticity/learning/memory)*. *89*, 4363–4367.

Euston, D. R., Gruber, A. J., & Mcnaughton, B. L. (2012). The Role of Medial Prefrontal Cortex in Memory and Decision Making. *Neuron*, *76*, 1057–1070. https://doi.org/10.1016/j.neuron.2012.12.002

Felix-Ortiz, A. C., Burgos-Robles, A., Bhagat, N. D., Leppla, C. A., & Tye, K. M. (2016). Bidirectional modulation of anxiety-related and social behaviors by amygdala projections to the medial prefrontal cortex. *Neuroscience*, *321*, 197–209. https://doi.org/10.1016/J.NEUROSCIENCE.2015.07.041

Finn, A. S., Sheridan, M. A., Hudson Kam, C. L., Hinshaw, S., & D'Esposito, M. (2010). Longitudinal Evidence for Functional Specialization of the Neural Circuit Supporting Working Memory in the Human Brain. *Journal of Neuroscience*, *30*(33), 11062–11067. https://doi.org/10.1523/JNEUROSCI.6266-09.2010

Floresco, S. B., Braaksma, D. N., & Anthony, G. Phillips. (1982). Thalamic–cortical–striatal circuitry subserves working memory during delayed responding on a radial arm maze. *Journal of Neuroscience*, *19*(24), 11061–11071.

Forbes, N. F., Carrick, L. A., McIntosh, A. M., & Lawrie, S. M. (2009). Working memory in schizophrenia: a meta-analysis. *Psychological Medicine*, *39*(6), 889–905. https://doi.org/10.1017/S0033291708004558

Forsberg, M., Seth, H., Björefeldt, A., Lyckenvik, T., Andersson, M., Wasling, P., Zetterberg, H., & Hanse, E. (2019). Ionized calcium in human cerebrospinal fluid and its influence on intrinsic and synaptic excitability of hippocampal pyramidal neurons in the rat. *Journal of Neurochemistry*, *149*(4), 452–470. https://doi.org/10.1111/JNC.14693

Friedrich, J., Urbanczik, R., & Senn, W. (2011). Spatio-Temporal Credit Assignment in Neuronal Population Learning. *PLOS Computational Biology*, *7*(6), e1002092. https://doi.org/10.1371/JOURNAL.PCBI.1002092

Gabbott, P. L. A., Warner, T. A., Jays, P. R. L., Salway, P., & Busby, S. J. (2005). Prefrontal cortex in the rat: Projections to subcortical autonomic, motor, and limbic centers. *Journal of Comparative Neurology*, *492*(2), 145–177. https://doi.org/10.1002/CNE.20738

Gale, G. D., Anagnostaras, S. G., Godsil, B. P., Mitchell, S., Nozawa, T., Sage, J. R., Wiltgen, B., & Fanselow, M. S. (2004). Role of the Basolateral Amygdala in the Storage of Fear Memories across the Adult Lifetime of Rats. *Journal of Neuroscience*, *24*(15), 3810–3815. https://doi.org/10.1523/JNEUROSCI.4100-03.2004

Gerstner, W., Lehmann, M., Liakoni, V., Corneil, D., & Brea, J. (2018). Eligibility Traces and Plasticity on Behavioral Time Scales: Experimental Support of NeoHebbian Three-Factor Learning Rules. *Frontiers in Neural Circuits*, *12*, 53. https://doi.org/10.3389/FNCIR.2018.00053/BIBTEX

Ghods-Sharifi, S., St. Onge, J. R., & Floresco, S. B. (2009). Fundamental Contribution by the Basolateral Amygdala to Different Forms of Decision Making. *Journal of Neuroscience*, *29*(16), 5251–5259. https://doi.org/10.1523/JNEUROSCI.0315-09.2009

Gilboa, A., Winocur, G., Grady, C. L., Hevenor, S. J., & Moscovitch, M. (2004). Remembering Our Past: Functional Neuroanatomy of Recollection of Recent and Very Remote Personal Events. *Cerebral Cortex*, *14*(11), 1214–1225. https://doi.org/10.1093/CERCOR/BHH082

Godsil, B. P., Kiss, J. P., Spedding, M., & Jay, T. M. (2013). The hippocampal–prefrontal pathway: The weak link in psychiatric disorders? *European Neuropsychopharmacology*, *23*(10), 1165–1181. https://doi.org/10.1016/J.EURONEURO.2012.10.018

Guillery, R. W., & Sherman, S. M. (2002). The thalamus as a monitor of motor outputs. *Philosophical Transactions of the Royal Society of London. Series B: Biological Sciences*, *357*(1428), 1809–1821. https://doi.org/10.1098/RSTB.2002.1171

He, K., Huertas, M., Hong, S. Z., Tie, X. X., Hell, J. W., Shouval, H., & Kirkwood, A. (2015). Distinct Eligibility Traces for LTP and LTD in Cortical Synapses. *Neuron*, *88*(3), 528–538. https://doi.org/10.1016/J.NEURON.2015.09.037

Hebb, D. 0. (1949). The Organization of Behavior A NEUROPSYCHOLOGICAL THEORY. *Wiley*.

Heidbreder, C. A., & Groenewegen b, H. J. (2003). The medial prefrontal cortex in the rat: evidence for a dorso-ventral distinction based upon functional and anatomical characteristics. *Neuroscience & Biobehavioral Reviews*, *27*(6), 555–579.

Herring, B. E., & Nicoll, R. A. (2016). Long-Term Potentiation: From CaMKII to AMPA Receptor Trafficking. *Annual Review of Physiology*, *78*(Volume 78, 2016), 351–365. https://doi.org/10.1146/ANNUREV-PHYSIOL-021014-071753/CITE/REFWORKS

Herry, C., Ciocchi, S., Senn, V., Demmou, L., Müller, C., & Lüthi, A. (2008). Switching on and off fear by distinct neuronal circuits. *Nature 2008 454:7204*, *454*(7204), 600–606. https://doi.org/10.1038/nature07166

Hoover, W. B., & Vertes, R. P. (2007). Anatomical analysis of afferent projections to the medial prefrontal cortex in the rat. *Brain Structure and Function*, *212*(2), 149–179. https://doi.org/10.1007/S00429-007-0150-4/FIGURES/12

Hunt, P. R., & Aggleton, J. P. (1991). Medial dorsal thalamic lesions and working memory in the rat. *Behavioral and Neural Biology*, *55*(2), 227–246.

Irwin, L. N., Kofler, M. J., Soto, E. F., & Groves, N. B. (2019). Do children with attention-deficit/hyperactivity disorder (ADHD) have set shifting deficits? *Neuropsychology*, *33*(4), 470. https://doi.org/10.1037/neu0000546

Izquierdo, A., Brigman, J. L., Radke, A. K., Rudebeck, P. H., & Holmes, A. (2017). The neural basis of reversal learning: An updated perspective. *Neuroscience*, *345*, 12–26. https://doi.org/10.1016/J.NEUROSCIENCE.2016.03.021

James, W. (1890). The principles of psychology. *The Principles of Psychology.* https://doi.org/10.1037/11059-000

Jones, H. C., & Keep, R. F. (1988). Brain fluid calcium concentration and response to acute hypercalcaemia during development in the rat. *The Journal of Physiology*, *402*(1), 579–593. https://doi.org/10.1113/JPHYSIOL.1988.SP017223

Kauer, J. A., & Malenka, R. C. (2007). Synaptic plasticity and addiction. *Nature Reviews Neuroscience 2007 8:11*, *8*(11), 844–858. https://doi.org/10.1038/nrn2234

Kelly, C. J., & Martina, M. (2018). Circuit-selective properties of glutamatergic inputs to the rat prelimbic cortex and their alterations in neuropathic pain. *Brain Structure and Function*, *223*(6), 2627–2639. https://doi.org/10.1007/S00429-018-1648-7/FIGURES/8

Kennedy, M. (2016). Synaptic signaling in learning and memory. *Cold Spring Harbor Perspectives in Biology*, *8*(2). https://doi.org/10.1101/cshperspect.a016824

Kim, J., Pignatelli, M., Xu, S., Itohara, S., & Tonegawa, S. (2016). Antagonistic negative and positive neurons of the basolateral amygdala. *Nature Neuroscience 2016 19:12*, *19*(12), 1636–1646. https://doi.org/10.1038/nn.4414

Klopf, H. (1972). *Brain Function and Adaptive Systems: A Heterostatic Theory*.

Lee, A. T., Gee, S. M., Vogt, D., Patel, T., Rubenstein, J. L., & Sohal, V. S. (2014). Pyramidal Neurons in Prefrontal Cortex Receive Subtype-Specific Forms of Excitation and Inhibition. *Neuron*, *81*(1), 61–68. https://doi.org/10.1016/J.NEURON.2013.10.031

Lisman, J., Schulman, H., & Cline, H. (2002). The molecular basis of CaMKII function in synaptic and behavioural memory. *Nature Reviews Neuroscience 2002 3:3*, *3*(3), 175–190. https://doi.org/10.1038/nrn753

Lisman, J., & Spruston, N. (2005). Postsynaptic depolarization requirements for LTP and LTD: a critique of spike timing-dependent plasticity. *Nature*, *8*(7).

Lisman, J., & Spruston, N. (2010). Questions about STDP as a general model of synaptic plasticity. *Frontiers in Synaptic Neuroscience*, *OCT*, 1–5. https://doi.org/10.3389/FNSYN.2010.00140/FULL

Lisman, J., Yasuda, R., & Raghavachari, S. (2012). Mechanisms of CaMKII action in long-term potentiation. *Nature Reviews Neuroscience 2012 13:3*, *13*(3), 169–182. https://doi.org/10.1038/nrn3192

Little, J. P., & Carter, A. G. (2013). Synaptic Mechanisms Underlying Strong Reciprocal Connectivity between the Medial Prefrontal Cortex and Basolateral Amygdala. *Journal of Neuroscience*, *33*(39), 15333–15342. https://doi.org/10.1523/JNEUROSCI.2385-13.2013

Liu, X., & Carter, A. G. (2018a). Ventral Hippocampal Inputs Preferentially Drive Corticocortical Neurons in the Infralimbic Prefrontal Cortex. *The Journal of Neuroscience : The Official Journal of the Society for Neuroscience*, *38*(33), 7351–7363. https://doi.org/10.1523/JNEUROSCI.0378-18.2018

Liu, X., & Carter, A. G. (2018b). Ventral Hippocampal Inputs Preferentially Drive Corticocortical Neurons in the Infralimbic Prefrontal Cortex. *Journal of Neuroscience*, *38*(33), 7351–7363. https://doi.org/10.1523/JNEUROSCI.0378-18.2018

Llinás, R., Sugimori, M., & Silver, R. B. (1992). Microdomains of High Calcium Concentration in a Presynaptic Terminal. *Science*, *256*(5057), 677–679. https://doi.org/10.1126/SCIENCE.1350109

Lü Scher, C., Malenka, R. C., Sheng, M., Sabatini, B., & Sü, T. C. (2012). NMDA Receptor-Dependent Long-Term Potentiation and Long-Term Depression (LTP/LTD). *Cold Spring Harbor Perspectives in Biology*, *4*(6), a005710. https://doi.org/10.1101/CSHPERSPECT.A005710

Magee, J. C., & Johnston, D. (1997). A Synaptically Controlled, Associative Signal for Hebbian Plasticity in Hippocampal Neurons. *Science*, *275*(5297), 209–213. https://doi.org/10.1126/SCIENCE.275.5297.209

Malinow, R., & Malenka, R. C. (2003). AMPA Receptor Trafficking and Synaptic Plasticity. *Annual Review of Neuroscience*, *25*, 103–126. https://doi.org/10.1146/ANNUREV.NEURO.25.112701.142758

Manoocheri, K., & Carter, A. G. (2022). Rostral and caudal basolateral amygdala engage distinct circuits in the prelimbic and infralimbic prefrontal cortex. *ELife*, *11*. https://doi.org/10.7554/ELIFE.82688

Marek, R., & Sah, P. (2018). Neural circuits mediating fear learning and extinction. *Advances in Neurobiology*, *21*, 35–48. https://doi.org/10.1007/978-3-319-94593-4_2/FIGURES/2

Markram, H., Gerstner, W., & Sjöström, P. J. (2011). A history of spike-timing-dependent plasticity. *Frontiers in Synaptic Neuroscience*, *3*(AUG), 1–24. https://doi.org/10.3389/FNSYN.2011.00004/BIBTEX

Markram, H., Lübke, J., Frotscher, M., & Sakmann, B. (1997). Regulation of Synaptic Efficacy by Coincidence of Postsynaptic APs and EPSPs. *Science*, *275*(5297), 213–215. https://doi.org/10.1126/SCIENCE.275.5297.213

Markram, H., Lubke, J., Michael, F., & Bert, S. (1997). Regulation of Synaptic Efficacy by Coincidence of Postsynaptic APs and EPSPs. *Science*, *275*, 213–215.

Marlin, J. J., & Carter, A. G. (2014). GABA-A receptor inhibition of local calcium signaling in spines and dendrites. *Journal of Neuroscience*, *34*(48), 15898–15911. https://doi.org/10.1523/JNEUROSCI.0869-13.2014

Martin, S. J., Grimwood, P. D., & Morris, R. G. M. (2000). Synaptic plasticity and memory: An evaluation of the hypothesis. *Annual Review of Neuroscience*, *23*(Volume 23, 2000), 649–711. https://doi.org/10.1146/ANNUREV.NEURO.23.1.649/CITE/REFWORKS

McTeague, L. M., Rosenberg, B. M., Lopez, J. W., Carreon, D. M., Huemer, J., Jiang, Y., Chick, C. F., Eickhoff, S. B., & Etkin, A. (2020). Identification of common neural circuit disruptions in emotional processing across psychiatric disorders. *American Journal of Psychiatry*, *177*(5), 411–421. https://doi.org/10.1176/APPI.AJP.2019.18111271/ASSET/IMAGES/LARGE/APPI.AJP.2019.18111271F5.JPEG

M'harzi, M., Jarrard, L. E., Willig, F., Palacios, A., & Delacour, J. (1991). Selective fimbria and thalamic lesions differentially impair forms of working memory in rats. *Behavioral and Neural Biology*, *56*(3), 221–239.

Milad, M., & Quirk, G. J. (n.d.). Neurons in medial prefrontal cortex signal memory for fear extinction. *Nature.ComMR Milad, GJ QuirkNature, 2002•nature.Com*.

Miller, E. K., & Cohen, J. D. (2001). An integrative theory of prefrontal cortex function. *Annual Review of Neuroscience*, *24*(Volume 24, 2001), 167–202. https://doi.org/10.1146/ANNUREV.NEURO.24.1.167/CITE/REFWORKS

Minzenberg, M. J., Laird, A. R., Thelen, S., Carter, C. S., & Glahn, D. C. (2009). Meta-analysis of 41 Functional Neuroimaging Studies of Executive Function in Schizophrenia. *Archives of General Psychiatry*, *66*(8), 811–822. https://doi.org/10.1001/ARCHGENPSYCHIATRY.2009.91

Mitchell, A. S., & Chakraborty, S. (2013). What does the mediodorsal thalamus do? *Frontiers in Systems Neuroscience*, *7*(37). https://doi.org/10.3389/FNSYS.2013.00037/FULL

Mulkey, R., & Malenka, R. (1992). Mechanisms underlying induction of homosynaptic long-term depression in area CA1 of the hippocampus. *Neuron*.

Nicoll, R. A., Kauer, J. A., & Malenka, R. C. (1988). The current excitement in long-term potentiation. *Neuron*, *1*(2), 97–103. https://doi.org/10.1016/0896-6273(88)90193-6

Padilla-Coreano, N., Bolkan, S. S., Pierce, G. M., Blackman, D. R., Hardin, W. D., Garcia-Garcia, A. L., Spellman, T. J., & Gordon, J. A. (2016). Direct Ventral Hippocampal-Prefrontal Input Is Required for Anxiety-Related Neural Activity and Behavior. *Neuron*, *89*(4), 857–866. https://doi.org/10.1016/J.NEURON.2016.01.011

Parnaudeau, S., Bolkan, S. S., & Kellendonk, C. (2018). The Mediodorsal Thalamus: An Essential Partner of the Prefrontal Cortex for Cognition. *Biological Psychiatry*, *83*(8), 648–656. https://doi.org/10.1016/J.BIOPSYCH.2017.11.008

Parnaudeau, S., O'neill, P.-K., Bolkan, S. S., Ward, R. D., Abbas, A. I., Roth, B. L., Balsam, P. D., Gordon, J. A., & Kellendonk, C. (2013). Inhibition of mediodorsal thalamus disrupts thalamofrontal connectivity and cognition. *Neuron*, *77*(6), 1151-1162. https://doi.org/10.1016/j.neuron.2013.01.038

Peters, J., Dieppa-Perea, L. M., Melendez, L. M., & Quirk, G. J. (2010). Induction of fear extinction with hippocampal-lnfralimbic BDNF. *Science*, *328*(5983), 1288–1290. https://doi.org/10.1126/SCIENCE.1186909/SUPPL_FILE/PETERS.SOM.PDF

Ramon Cajal, S. (1894). The Croonian lecture.—La fine structure des centres nerveux. *Proceedings of the Royal Society of London*, *55*(331–335), 444–468. https://doi.org/10.1098/RSPL.1894.0063

Rauch, S. L., Shin, L. M., & Wright, C. I. (2003). Neuroimaging Studies of Amygdala Function in Anxiety Disorders. *Annals of the New York Academy of Sciences*, *985*(1), 389–410. https://doi.org/10.1111/J.1749-6632.2003.TB07096.X

Retchless, B., Gao, W., neuroscience, J. J.-N., & 2012, undefined. (2012). A single GluN2 subunit residue controls NMDA receptor channel properties via intersubunit interaction. *Nature.ComBS Retchless, W Gao, JW JohnsonNature Neuroscience, 2012•nature.Com*. https://doi.org/10.1038/nn.3025

Rose, J. E., & Woolsey, C. N. (1949). Organization of the mammalian thalamus and its relationships to the cerebral cortex. *Electroencephalography and Clinical Neurophysiology*, *1*(1–4), 391–404. https://doi.org/10.1016/0013-4694(49)90212-6

Schmitt, L. I., Wimmer, R. D., Nakajima, M., Happ, M., Mofakham, S., & Halassa, M. M. (2017). Thalamic amplification of cortical connectivity sustains attentional control. *Nature*, *545*(7653), 219–223. https://doi.org/10.1038/nature22073

Seeburg, P. H., & Hartner, J. (2003). Regulation of ion channel/neurotransmitter receptor function by RNA editing. *Current Opinion in Neurobiology*, *13*(3), 279–283. https://doi.org/10.1016/S0959-4388(03)00062-X

Sherrington, C. S. (1906). The Integrative Action of the Nervous System. In *The Journal of Nervous and Mental Disease*. Routledge. https://doi.org/10.4324/9781003009405-23/INTEGRATIVE-ACTION-NERVOUS-SYSTEM-CHARLES-SCOTT-SHERRINGTON

Siapas, A., Lubenov, E., & Wilson, M. (2005). Prefrontal phase locking to hippocampal theta oscillations. *Neuron*, *46*, 141–151. https://doi.org/10.1016/j.neuron.2005.02.028

Silver, R. A., Lamb, A. G., & Bolsover, S. R. (1990). Calcium hotspots caused by L-channel clustering promote morphological changes in neuronal growth cones. *Nature 1990 343:6260*, *343*(6260), 751–754. https://doi.org/10.1038/343751a0

Spellman, T., Rigotti, M., Ahmari, S. E., Fusi, S., Gogos, J. A., & Gordon, J. A. (2015). Hippocampal–prefrontal input supports spatial encoding in working memory. *Nature 2015 522:7556*, *522*(7556), 309–314. https://doi.org/10.1038/nature14445

Spruston, N., Jaffe, D. B., & Johnston, D. (1994). Dendritic attenuation of synaptic potentials and currents: the role of passive membrane properties. *Trends in Neurosciences*, *17*(4), 161–166. https://doi.org/10.1016/0166-2236(94)90094-9

Squire, L. R. (1992). Declarative and Nondeclarative Memory: Multiple Brain Systems Supporting Learning and Memory. *Journal of Cognitive Neuroscience*, *4*(3), 232–243. https://doi.org/10.1162/JOCN.1992.4.3.232

Suvrathan, A. (2018). Beyond STDP-towards diverse and functionally relevant plasticity rules This review comes from a themed issue on Neurobiology of learning and plasticity. *Current Opinion in Neurobiology*, *54*, 12–19. https://doi.org/10.1016/j.conb.2018.06.011

Thierry, A.-M., Gioanni, Y., Dégénétais, E., & Glowinski, J. (2000). *Hippocampo-Prefrontal Cortex Pathway: Anatomical and Electrophysiological Characteristics*. https://doi.org/10.1002/1098-1063

Tovote, P., Fadok, J. P., & Lüthi, A. (2015). Neuronal circuits for fear and anxiety. *Nature Reviews Neuroscience 2015 16:6*, *16*(6), 317–331. https://doi.org/10.1038/nrn3945

Traynelis, S. F., Wollmuth, L. P., McBain, C. J., Menniti, F. S., Vance, K. M., Ogden, K. K., Hansen, K. B., Yuan, H., Myers, S. J., & Dingledine, R. (2010). Glutamate Receptor Ion Channels: Structure, Regulation, and Function. *Pharmacological Reviews*, *62*(3), 405–496. https://doi.org/10.1124/PR.109.002451

Tripathi, A., Schenker, E., Spedding, M., & Jay, T. M. (2016). The hippocampal to prefrontal cortex circuit in mice: a promising electrophysiological signature in models for psychiatric disorders. *Brain Structure and Function*, *221*(4), 2385–2391. https://doi.org/10.1007/S00429-015-1023-X/FIGURES/3

Tse, D., Langston, R. F., Kakeyama, M., Bethus, I., Spooner, P. A., Wood, E. R., Witter, M. P., & Morris, R. G. M. (2007). Schemas and memory consolidation. *Science*, *316*(5821), 76–82. https://doi.org/10.1126/SCIENCE.1135935

Turrigiano, G. G., & Nelson, S. B. (2004). Homeostatic plasticity in the developing nervous system. *Nature Reviews Neuroscience 2004 5:2*, *5*(2), 97–107. https://doi.org/10.1038/nrn1327

Twining, R. C., Lepak, K., Kirry, A. J., & Gilmartin, M. R. (2020). Ventral Hippocampal Input to the Prelimbic Cortex Dissociates the Context from the Cue Association in Trace Fear Memory. *Journal of Neuroscience*, *40*(16), 3217–3230. https://doi.org/10.1523/JNEUROSCI.1453-19.2020

Van De Werd, H. J. J. M., Rajkowska, G., Evers, P., & Uylings, H. B. M. (2010). Cytoarchitectonic and chemoarchitectonic characterization of the prefrontal cortical areas in the mouse. *Brain Structure and Function*, *214*(4), 339–353. https://doi.org/10.1007/S00429-010-0247-Z/FIGURES/15

Vicini, S., Wang, J. F., Li, J. H., Zhu, W. J., Wang, Y. H., Luo, J. H., Wolfe, B. B., & Grayson, D. R. (1998). Functional and pharmacological differences between recombinant N- methyl-D-aspartate receptors. *Journal of Neurophysiology*, *79*(2), 555–566. https://doi.org/10.1152/JN.1998.79.2.555

Yang, Y., & Wang, J. Z. (2017). From structure to behavior in basolateral amygdala-hippocampus circuits. *Frontiers in Neural Circuits*, *11*, 86. https://doi.org/10.3389/FNCIR.2017.00086/BIBTEX

Yehuda, R., & LeDoux, J. (2007). Response variation following trauma: a translational neuroscience approach to understanding PTSD. *Neuron*, *56*(1), 19–32. https://doi.org/10.1016/j.neuron.2007.09.006

Yoon, T., Okada, J., Jung, M. W., & Kim, J. J. (2008). Prefrontal cortex and hippocampus subserve different components of working memory in rats. *Learning & Memory*, *15*(3), 97–105. https://doi.org/10.1101/LM.850808

Young, H. L., Stevens, A. A., Converse, E., & Mair, R. G. (1996). A comparison of temporal decay in place memory tasks in rats (Rattus norvegicus) with lesions affecting thalamus, frontal cortex, or the hippocampal system. *Behavioral Neuroscience*, *110*(6), 1244.

Zhang, A., Yang, C., Li, G., Wang, Y., Liu, P. H., Liu, Z., Sun, N., & Zhang, K. (2020). Functional connectivity of the prefrontal cortex and amygdala is related to depression status in major depressive disorder. *Journal of Affective Disorders*, *274*, 897–902. https://doi.org/10.1016/J.JAD.2020.05.053